

## Biological Psychiatry

BPS-D-13-02168 R2

4/30/2014 10:01 PM

### **Coordinated mRNA/miRNA changes in fibroblasts of patients with major depression**

*Krassimira A. Garbett<sup>1,§</sup>, Andrea Vereczkei<sup>1,2,§</sup>, Sára Kálmán<sup>1,3</sup>,  
Jacquelyn A Brown<sup>1</sup>, Warren D. Taylor<sup>1</sup>, Gábor Faludi<sup>4</sup>,  
Željka Korade<sup>1,6</sup>, Richard C. Shelton<sup>5</sup> and Károly Mirnics<sup>1,3,6,\*</sup>*

<sup>1</sup> Department of Psychiatry, Vanderbilt University, Nashville, TN, USA

<sup>2</sup> Institute for Medical Chemistry, Molecular Biology and Pathobiochemistry, Semmelweis University, Budapest, Hungary

<sup>3</sup> Department of Psychiatry, University of Szeged, Szeged, Hungary

<sup>4</sup> Department of Psychiatry, Kútvölgyi Clinical Centre, Semmelweis University, Budapest, Hungary

<sup>5</sup> Department of Psychiatry, University of Alabama, Birmingham, AL, USA

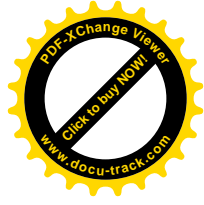
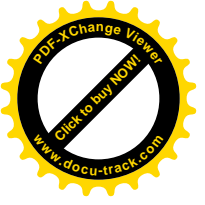
<sup>6</sup> Vanderbilt Kennedy Center for Research on Human Development, Vanderbilt University, Nashville, TN, USA

**Keywords:** human fibroblasts, major depression, miRNA, gene expression, DNA microarray, biomarker

Abstract: 235 words  
Tables: 2  
Figures: 3  
Supplementary Materials: 7  
Body Text: 4002 words

§ K.A.G and A.V. equally contributed to this study.

\*Correspondence: **Károly Mirnics**, Department of Psychiatry, Vanderbilt University, 8130A MRB III, 465 21st Avenue South, Nashville TN 37232, USA, [karoly.mirnics@vanderbilt.edu](mailto:karoly.mirnics@vanderbilt.edu), Office phone: 615-936-1074, <http://www.mirnicslab.org>



## ABSTRACT

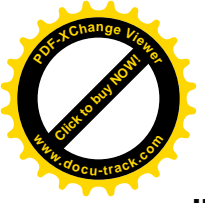
**Background:** Peripheral biomarkers for major psychiatric disorders have been an elusive target for the last half a century. Dermal fibroblasts are a simple, relevant, and much underutilized model for studying molecular processes of patients with affective disorders as they share considerable similarity of signal transduction with neuronal tissue.

**Methods:** Cultured dermal fibroblast samples from patients with Major Depressive Disorder (MDD) and matched controls (CNTR) (n=16 pairs, 32 samples) were assayed for genome wide mRNA expression using microarrays. In addition, a simultaneous qPCR-based assessment of >1,000 miRNA species was performed. Finally, to test the relationship between the mRNA-miRNA expression changes, the two datasets were correlated with each other.

**Results:** Our data revealed that MDD fibroblasts, when compared to matched controls, showed a strong mRNA gene expression pattern change in multiple molecular pathways, including cell-to-cell communication, innate/adaptive immunity and cell proliferation. Furthermore, the same patient fibroblasts showed altered expression of a distinct panel of 38 miRNAs, which putatively targeted many of the differentially expressed mRNAs. The miRNA-mRNA expression changes appeared to be functionally connected, as the majority of the miRNA and mRNA changes were in the opposite direction.



**Conclusions:** Our data suggest that a combined miRNA-mRNA assessments are informative about the disease process, and that analyses of dermal fibroblasts might lead to the discovery of promising peripheral biomarkers of MDD, which could be potentially used to aid the diagnosis and allow mechanistic testing of disturbed molecular pathways.



## INTRODUCTION:

There has been an intensive search for peripheral biomarkers of major psychiatric disorders for the last half a century. These efforts encompassed gene expression profiling of peripheral mononuclear cells (1, 2), biochemical evaluations of serum (3), urine (4), saliva (5), and cerebrospinal fluid (6), gene association studies of DNA markers (7) and many other approaches. More recently, inducible pluripotent stem cells (iPSCs) emerged as a very promising model for studying neuronal lineage disturbances across various disorders (8-10). Unfortunately, the complex diagnostic-phenotypic-genetic-etiological heterogeneity continues (11) to provide significant obstacles for identifying highly specific and sensitive peripheral biomarkers of mental disorders.

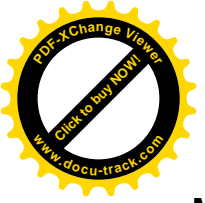
Transcriptome profiling experiments of postmortem human brain tissue from subjects with major depressive disorder (MDD) suggest evidence of local inflammatory, apoptotic, oxidative stress and multiple other, non-brain specific molecular processes (12-17). Emerging evidence argues that many of these changes might be, at least partially, driven by altered expression of microRNAs (miRNAs): miRNA levels change during stress, in the brain of animal models of depression, and in human postmortem brain of MDD subjects (18) and depressed suicide subjects (19).

Importantly, peripheral biomarker studies of MDD over the last several decades revealed that peripheral growth factors, pro-inflammatory cytokines, endocrine factors, and metabolic markers all contribute to the disease pathophysiology (20). These combined data suggest that MDD is not only a disease of the CNS, but affects the



whole body (21, 22), and that peripheral cellular-molecular events are strongly correlated with the disease pathology in the CNS (23). Experimental data suggest that analyzing patient dermal fibroblasts is a simple, relevant, and much underutilized model for studying processes of signal transduction in patients with affective disorders (24-26). Dermal fibroblasts are easy to establish and maintain in culture without transformation, and the majority of confounding factors (e.g. life style or medication use) are virtually eliminated after several rounds of cell division. Furthermore, a recent study of fibroblasts obtained from MDD patients highlights the role that oxidative stress might play in the pathophysiology of MDD (25), which has been already well-established across multiple other research models and patient populations (27, 28). Thus, analyzing dermal fibroblast cultures from patients can give us meaningful insights into the molecular effects of the combined genetic predisposition to the disorder.

It appears that biomarker panels hold a greater promise than single analyte molecules in aiding the diagnosis, monitoring disease progression or therapeutic response in MDD (20). As understanding non-neuronal changes in MDD can be informative of the overall disease pathophysiology (23), we performed a combined mRNA-miRNA profiling of dermal fibroblasts from patients with MDD and matched controls.



## METHODS AND MATERIALS:

### Participants in the study

The Study was approved by the Vanderbilt University Institutional Review Board (IRB). Procedures for recruitment and diagnosis have been described previously (24, 25). All participants were diagnosed with a current Major Depressive Episode according to the Structured Clinical Interview for DSM-IV-TR (29) with an exclusion criteria of other primary axis I DSM-IV diagnosis. A written informed consent was obtained from all participants before collecting skin biopsy samples. Sixteen pairs of subjects with Major Depressive Disorder (MDD) and healthy controls (CNTR) were matched by age, race and sex. The average age of the MDD patients and CNTR were comparable (MDD=34.9, CNTR=35.2), as were the sex (12F/4M in both groups) and race (12W/4AA), but there was a significant difference in body mass index at the time of skin biopsy (25.4 in CNTR and 32.3 in MDD,  $p=0.03$ ) (**Supplemental Material 1**).

### Human dermal fibroblasts

The skin biopsy was obtained from the lateral side of the upper arm (1 x 2 mm) according to a protocol previously described in details (24, 25). The sample was put into regular Dulbecco's Modified Eagle's Medium (DMEM, MediaTech, Manassas, VA, USA) without serum and processed the same day. Briefly, biopsy sample was cut into several smaller pieces with scissors and incubated in trypsin and collagenase mix at 37°C for 1 hr. Regular medium was added [DMEM containing high glucose, L-glutamine, 10% fetal bovine serum (FBS, ThermoScientific HyClone, Logan, UT, USA), and Penicillin/Streptomycin solution (MediaTech)] and biopsy pieces with dissociated cells were pelleted by centrifugation. The supernatant was discarded. Biopsy pieces with



cells were resuspended in fresh regular medium and transferred to 60 mm tissue culture plates. Cells were cultured in incubator at 37°C and 5% CO<sub>2</sub> concentration. Medium was changed 3 times a week. In about 2-3 weeks the fibroblasts divided and became confluent. The fibroblasts were subcultured using 0.5% Trypsin-EDTA (Invitrogen) as described elsewhere (30) and expanded for freezing in a liquid nitrogen cell repository or expanded for experiments. Selected fibroblasts from matching patient/control pairs were cultured simultaneously to ensure they grow under the same conditions. Cell growth and proliferation were checked regularly during the whole experiment. All cultured fibroblasts were less than passage 15. At the end of experiment, the fibroblasts were washed 2X with ice-cold PBS, collected with cell scraper, pelleted by centrifugation and frozen on dry ice and stored at -80°C.

#### **mRNA expression analysis by microarrays**

Total RNA was isolated using the *mirVana*<sup>™</sup> miRNA Isolation Kit (Ambion, Foster City, CA, USA) and RNA quality assessed by an Agilent 2100 Bioanalyzer (Agilent, Palo Alto, California, USA). cDNA was generated using 2 µg of total RNA. cDNA synthesis, amplification and labeling were performed using The Enzo Life Sciences Single-Round RNA Amplification and Biotin Labeling System (Enzo Life Sciences, Farmingdale, NY, USA). 5 µg of the biotin labeled, fragmented aRNA were hybridized to a GeneChip HT HG-U133+ PM Array Plate (Affymetrix Inc, Santa Clara, CA, USA) at the Vanderbilt Microarray Shared Resource core facility.

Segmented images from each microarray were normalized and log<sub>2</sub> transformed using GC-robust multi-array analysis (GC-RMA) (31). The normalized expression values were used in all analyses. Average expression values for each group (MDD and CNTR)



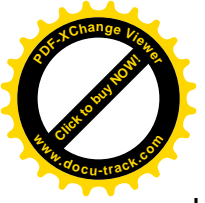
were calculated for each gene probe. The magnitude of expression change was determined by the Average Logarithmic Ratio ( $ALR = \text{mean}_{MDD} - \text{mean}_{CNTR}$ ). Student's paired and grouped two-tailed t-tests were used to test the significance of the difference in gene expression (32-36). A gene was considered to be differentially expressed between MDD and CNTR when it met the dual criteria of  $|ALR| > 0.585$  (50%) and both pairwise and groupwise  $p$ -values  $< 0.05$ .

The differentially expressed genes were subjected to a two-way hierarchical clustering analysis based on Pearson correlation using GenePattern software (37). Gene set enrichment analysis (GSEA) based on pre-defined gene classes were carried out with the GenePattern software (38). GSEA determines whether an *a priori* defined set of genes shows statistically significant, concordant differences between our subject groups based on the BioCarta defined molecular pathways. GSEA calculates a *normalized enrichment score (NES)*, which reflects the degree to which a gene set is overrepresented in the ranked list of genes and a *nominal p-value* which estimates the statistical significance of the enrichment score for a single gene set. BioCarta gene sets were considered differentially expressed at *nominal p-value*  $< 0.05$ .

### **mRNA data validation by qPCR**

cDNA was generated with random primers using High Capacity cDNA Reverse Transcription Kit (Applied Biosystems, Foster City, CA). Primers for 13 genes (heparin-binding EGF-like growth factor - HBEGF, major histocompatibility complex, class II invariant chain - CD74, major histocompatibility complex, class II, DP alpha 1 – HLA-DPA1, glutathione S-transferase theta 1 - GSTT1, major histocompatibility complex, class II, DR alpha - HLA-DRA, major histocompatibility complex, class II, DQ beta 1 -



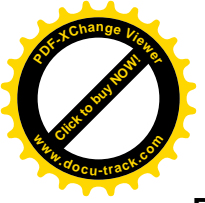


HLA-DQB1, major histocompatibility complex, class II, DP beta 1 - HLA-DPB1, major histocompatibility complex, class II, DQ alpha 1 - HLA-DQA1, interleukin 11 - IL11, Met proto-oncogene - MET, protocadherin 10 - PCDH10, S100 calcium binding protein B - S100B, tumor necrosis factor receptor superfamily, member 19 – TNF19) with efficiency >85% were used in SYBR Green based PCR reactions. Each sample was tested in 4 technical replicates on an ABI Prism 7300 thermal cycler (Applied Biosystems, Foster City, CA). The cycle threshold (Ct) of the housekeeping gene Glyceraldehyde-3-Phosphate Dehydrogenase (GAPDH) was used for normalization of all samples.

### **miRNome Arrays and qPCR validation**

Small RNAs were isolated using the *mirVana*<sup>TM</sup> miRNA Isolation Kit (Ambion, Foster City, CA, USA), and cDNA was prepared from it with miScript II RT Kit (Qiagen, Valencia, CA, USA) using miScript HiSpec Buffer. The individual sample cDNAs were pooled in equal proportions into four groups based on gender and age (**Supplemental Material 1**). The levels of 1008 miRNAs were assessed with Human miRNome *miScript miRNA PCR* Array (Qiagen, Valencia, CA, USA) according to the manufacturer's instructions and as previously described (26). A 30% difference between the average  $\Delta C_t$  for MDD and CNTR ( $|\Delta\Delta C_t| > 0.3785$ ) and a group-wise p-value generated by a ttest ( $p < 0.05$ ) were used to determine differential expression for each miRNA.

Custom generated miScript miRNA PCR Arrays (Qiagen, Valencia, CA, USA) were used to assay the level of seven miRNAs: hsa-miR-21, hsa-miR-377, hsa-miR-193a-3p, hsa-miR-542-3p, hsa-miR-22, hsa-miR-103a, hsa-miR-185. This assessment was performed on all individual samples (MDD n=16; CNTR n=16).

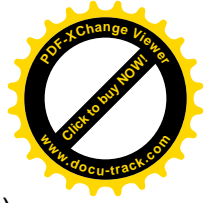
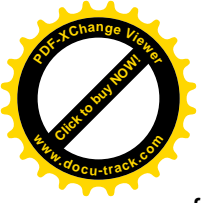


## RESULTS:

### mRNA signature in MDD fibroblasts

The experimental design for our study is presented in **Supplemental Material 2**. In the first part of the study, cultured fibroblast samples from patients with Major Depressive Disorder (MDD) and matched control (CNTR) subjects (n=16 pairs, 32 individuals) (**Supplemental Material 1**) were assayed for differential gene expression using *GeneChip* HT HG-U133 Plus PM 96 Array Plate (Affymetrix Inc, Santa Clara, CA). We identified 162 differentially expressed gene probes (**Supplemental Material 3**) that reported > 50% change, and  $p < 0.05$  in both pairwise and groupwise assessment. Of the 162 changed gene probes, representing 139 unique known genes, 25 showed increased expression and 114 had decreased levels in MDD, suggesting a predominant loss of function, rather than induction of gene expression in the diseased subjects. A two-way hierarchical clustering (*genes*  $\times$  *samples*) of the expression levels of these gene probes resulted in separation the majority of MDD samples to a distinct class (**Supplemental Material 4**).

Among the individual genes with the most prominent decrease were protocadherin 10 (PCDH10) (ALR= -1.73, ppval=0.00154, gpval=0.00057), tenascin XB (TNXB) (ALR=-1.30, ppval=0.04545, gpval=0.02515), periplakin (PPL) (ALR=-1.34, ppval=0.00556, gpval=0.02714), and hepatocyte growth factor receptor met (MET) (ALR=-1.21, ppval=0.04474, gpval=0.0012), which are involved in cell-cell communication/adhesion. Of these, due to its known effects on brain development and function, MET attracted particular attention and we decided to assess the expression of genes belonging to the MET intracellular cascade defined by Biocarta in a targeted



fashion. Overall, from the 37 genes 16 showed a significant difference (**Figure 1**) including phosphoinositide-3-kinase, regulatory subunit 1 (PIK3R1), hepatocyte growth factor (HGF), GRB2-associated binding protein 1 (GAB1), son of sevenless homolog 1 (SOS1), Rap guanine nucleotide exchange factor 1 (RAPGEF1), signal transducer and activator of transcription 3 (STAT3) protein tyrosine phosphatase, non-receptor type 11 (PTPN11), p21/Cdc42/Rac1-activated kinase 1 (PAK1), mitogen-activated protein kinase 1 (MAPK1), v-crkl sarcoma virus CT10 oncogene homolog like (CRKL), jun oncogene (JUN), phosphoinositide-3-kinase, catalytic, alpha polypeptide (PTEN), member of RAS oncogene family (RAP1A) mitogen-activated protein kinase kinase 1 (MAP2K1), and v-Ha-ras Harvey rat sarcoma viral oncogene homolog (HRAS). Furthermore, HGF/MET morphogenic signaling synergizes with v-erb-b2 erythroblastic leukemia viral oncogene homolog 2 (ErbB2) to enhance cell motility (39), and our data also revealed a significant downregulation of ErbB2, further supporting the notion for a deficit in HGF/MET-mediated signaling in MDD fibroblasts.

In addition to a targeted MET pathway analysis, we also performed an unbiased pathway enrichment analysis using Gene Set Enrichment Analyses (38). Using this approach, we identified 10 differentially expressed BioCarta gene sets, six of which were upregulated and 4 were downregulated in MDD samples (**Table 1**). Interestingly, most of these molecular pathways were related to cell-to-cell communication and are known for their role in the adaptive and innate immune system. These pathway analyses argue that the primary gene expression disturbance in the fibroblasts of MDD patients is in the expression of immune response genes, which has been also reported in the postmortem brain tissue of patients with MDD (12).



### **qPCR validation of mRNA signature**

Fourteen of the differentially expressed mRNA species were selected for further validation by qPCR. The genes for validation were primarily chosen because of their involvement in the immune system response, a process that has been previously implicated in the pathophysiology of the disease. Twelve of fourteen selected transcripts showed similar, significant expression differences between the control and MDD samples by the two methods, with a high degree of correlation between the microarray-reported ALRs and qPCR-obtained  $\Delta\Delta\text{Ct}$ s ( $r=0.84$ ) (**Supplemental Material 5**), but did not show correlation with body mass index in either dataset. qPCR-reported expression differences between the control and MDD samples were as follows: CD74:  $\Delta\Delta\text{Ct}=2.29$ ,  $p=0.012$ ; HLA-DRA:  $\Delta\Delta\text{Ct} =1.61$ ,  $p=0.017$ ; HLA-DQB1:  $\Delta\Delta\text{Ct}=1.31$ ,  $p=0.018$ ; IL11:  $\Delta\Delta\text{Ct}=1.13$ ,  $p=0.017$ ; HLA-DPA1:  $\Delta\Delta\text{Ct}=1.08$ ,  $p=0.011$ ; S100B:  $\Delta\Delta\text{Ct}=1.05$ ,  $p=0.031$ ; HBEGF:  $\Delta\Delta\text{Ct}= 1.00$ ,  $p=0.010$ ; HLA-DPB1:  $\Delta\Delta\text{Ct}=0.43$ ,  $p=0.156$ ; HLA-DQA1:  $\Delta\Delta\text{Ct}=0.29$ ,  $p=0.285$ ; MET:  $\Delta\Delta\text{Ct}=-0.42$ ,  $p=0.043$ ; PCDH10:  $\Delta\Delta\text{Ct}=-0.91$ ,  $p=0.036$ ; TNF19:  $\Delta\Delta\text{Ct}=-1.11$ ,  $p=0.007$  and GSTT1:  $\Delta\Delta\text{Ct}=-3.77$ ,  $p=0.007$ .

### **miRNA signature in MDD fibroblasts**

miRNAs are important control elements in the fine-tuning of gene expression, and are capable of regulating extensive transcriptional networks (26, 40). Therefore, we further sought to determine if there was a disturbance of miRNA expression profile in MDD fibroblasts. Small RNA species were isolated from each fibroblast culture, cDNA was generated, pooled in 4 groups according to gender and age, and then used to probe Human MirNome arrays, containing assays for 1008 known human miRNAs (26). We observed that approximately 50% (561) of the tested miRNAs were expressed in

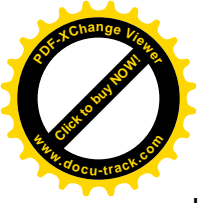


cultured dermal fibroblasts. We used a dual expression-significance criteria (26) for determining differential miRNA expression (>30% change,  $p < 0.05$ ). We detected 38 miRNAs with distinctly different expression in MDD fibroblasts compared to healthy controls (**Supplemental Material 6**). Of these, 17 miRNAs reported lower and 21 higher levels in MDD fibroblasts. Using unsupervised two-way hierarchical clustering of expression levels, these 38 miRNAs provided a clear separation basis of the MDD and CNTR samples (**Figure 2**).

Since the miRNA levels were assayed on 4 pooled sets of samples, we sought to validate the observed differences in individual samples. For this purpose, we created custom qPCR arrays containing assays for 7 differentially expressed miRNAs; hsa-miR-21\*, hsa-miR-377, hsa-miR-193a-3p, hsa-miR-542-3p, hsa-miR-22, hsa-miR-103a, hsa-miR-185. miRNA expression levels for these 7 miRNA species showed an extremely high correlation ( $R^2 = 0.93$ ,  $p < 0.001$ ) between the pooled sample and individual sample assessments, suggesting that the observations made using the combined samples were not an artifact generated by the pooling (**Figure 3**).

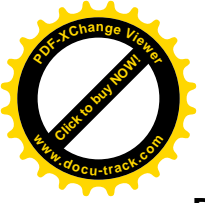
### **Cross-talk between miRNA and mRNA expression in MDD fibroblasts**

Next, we tested if the miRNA signature can explain some of the mRNA signature in MDD fibroblasts. To achieve this, we identified all predicted target genes/mRNAs for each of the 38 miRNAs using miRDB online database for miRNA target prediction and functional annotations (41),(42) and tested if the targeted mRNAs were enriched in the transcriptome profile of MDD fibroblasts (**Table 2**). 32 out of 38 miRNAs (89%) had at least one target mRNA that was differentially expressed between the MDD and control samples. Furthermore, 51% of the differentially expressed mRNAs were targets of at



least one of the 38 miRNAs that were differentially expressed in the MDD fibroblasts. These findings suggest that the miRNA-mRNA expression signatures of MDD fibroblasts are strongly interconnected.

miRNAs are most commonly considered negative regulators of mRNA expression (44, 45), so we hypothesized that the miRNA and their mRNA targets will show expression changes in the opposite direction. Indeed, we found that 28 (76%) of the miRNAs with altered expression had mRNA targets changed in the opposite direction. Acknowledging the fact that different prediction algorithms produce different sets of target genes, we also performed a secondary identification of miRNA targets using TargetScan Release 6.2 (<http://www.targetscan.org/>) (43). TargetScan identified miRNA targets (**Supplemental Material 7**) that were somewhat different from the ones identified by miRDB, but strikingly similar in terms of relating the miRNA and the mRNA changes in MDD; 65% (TargetScan) and 76% (MiRDB) of the differentially changed miRNAs had mRNA targets that were changed in the opposite direction. Regardless of these differences, the findings across the two databases suggest a functionally interconnected miRNA-mRNA network disturbance in MDD fibroblasts, where many (if not the majority) of the mRNA changes are miRNA driven. Nevertheless, it remains challenging to establish which specific miRNA species control what individual mRNA transcripts, as 64% of the differentially expressed mRNAs in MDD fibroblasts were hypothetically controlled by more than one miRNA.



## DISCUSSION:

Our data revealed that 1) MDD fibroblasts, when compared to matched controls, show a strong mRNA gene expression difference in molecular networks known to engage in cell-to-cell communication and innate/adaptive immunity; 2) the same patient fibroblasts showed altered expression in a distinct panel of 38 miRNAs, which appeared to target many of the differentially expressed mRNAs; 3) the miRNA-mRNA expression changes appeared to be functionally connected, as the majority of the miRNA and mRNA changes were in the opposite direction.

These findings have conceptual implications for our understanding of MDD pathophysiology. Our findings reinforce the notion that MDD is not only a disease of the brain, but molecular deficiencies in MDD patients are detectable in other peripheral organs (28, 46), including dermal fibroblasts. In addition, it is important to note that the observed mRNA and miRNA changes in the patient fibroblasts are most likely driven by genetic susceptibility to the disease, rather than effects of the environment and lifestyle: most of the epigenetic changes, environmental influences and drug effects are likely to disappear over time, as the fibroblasts continuously divide in the culture (25, 26). However, our experiments cannot exclude the possibility that some of the extremely stable, cell-division-resistant epigenetic factors might also contribute to the observed changes (47, 48). In summary, the molecular changes observed in cultured fibroblasts of MDD patients can provide us clues about lifestyle- and medication-independent, conserved disturbances in MDD across the various tissue types.

An unexpected and interesting finding of this study is the strikingly different level of expression of approximately half of the Biocarta defined hepatocyte growth factor



receptor *met* (MET) pathway genes. MET is a receptor tyrosine kinase activated by the hepatocyte growth factor (HGF) and affecting cellular signaling pathways involved in control of proliferation, motility, migration and invasion. Although the functions of MET have been primarily studied in the context of cancer (49), MET signaling is also known to be important in brain development (50) and the regulation of immune cells (51). Importantly, in a recent study HGF was the most highly associated plasma analyte with depressive symptoms (52). Furthermore, the *met* pathway facilitates adult neurogenesis (53), a process that is significantly impaired in major depression (54).

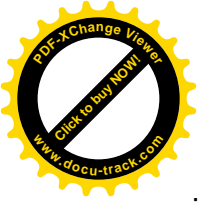
Immune system disturbances in MDD appear to be an integral part of the disease process (22, 55, 56). The overlap between symptoms of infectious diseases and common affective manifestations (57) suggested a shared pathophysiology between these two systems, which was investigated in a host of follow-up studies. Ultimately, the combined findings lead to the formulation of the inflammatory and neurodegenerative (I&ND) hypothesis of MDD (46), which states that MDD is a consequence of neurodegeneration and reduced neurogenesis that arise from inflammation and cell-mediated immune activation. Today, this view is supported by converging data obtained across different methods and systems. First, postmortem findings identified that MDD patients show a strong dysregulation of immune system pathways in the brain, encompassing altered levels of pro- and anti-inflammatory cytokine expression of IL-1 $\alpha$ , IL-2, IL-3, IL-5, IL-8, IL-9, IL-10, IL-12A, IL-13, IL-15, IL-18, IFN- $\gamma$  and lymphotoxin- $\alpha$  (12). Similarly, altered mRNA levels of immune system genes were found in the neocortex of subjects who committed suicide (58, 59). Second, the immune deficits appear to be systemic in patients with MDD, and that they are readily detectable in the





peripheral tissues (2). Inflammation and immune system biomarkers of MDD might include C-reactive protein (CRP), cytokines (in particular tumor necrosis factor- $\alpha$  (TNF- $\alpha$ ) and interleukin-6 (IL-6)), neopterin and tryptophan catabolites (reviewed by (28)). Third, while in the most recent genome-wide association study of MDD no SNPs achieved genome-wide significance in the MDD discovery or replication phase (60), candidate gene studies hint that genetic vulnerability in immune system genes might predispose to MDD in a complex pattern (61-64). However, it is also clear that the immune system genes are only partially responsible for the genetic vulnerability of MDD, as a recent pathway analysis found that genetic elements regulating growth and organ development might also represent vulnerability factors (65). Our results are also aligned with this overall view: the disturbance in classic complement pathway, cell-to-cell communication and innate/adaptive immunity suggest an integrated immune system and growth disturbance in the patient population.

Several miRNAs have been already associated with treatment response or an increased risk for major depression (18, 66-68). Recent reports suggest that polymorphism in the miR-30e precursor is associated with major depressive disorder risk (69), and that miRNA expression was significantly and globally down-regulated in prefrontal cortex of depressed suicide subjects (19). In addition, abnormal processing of pre-miR-182 (a circadian clock modulator) was found in major depression patients with insomnia (70). Unfortunately, due to lack of replication, specific experimental design, differences in analyzed tissue and variety of cohorts the data are challenging to interpret and combine into a comprehensive view in a context of MDD. However, it is clear that miRNAs play a pivotal role in a vast variety of MDD-relevant biological processes,



including synaptic plasticity, neurogenesis, and stress response (for a review, see (18)). Thus, it is worth pointing out that at least 8 of the 38 differentially expressed miRNAs that we identified in our MDD-fibroblast screen have been previously implicated in either pathophysiology of psychiatric disorders or pathophysiological processes relevant to MDD: 1) miR-32 and miR-22 levels were altered in both our and in a bipolar postmortem dataset (71), 2) miR-22 represses BDNF, serotonin receptor 2C (HTR2C), monoamine oxidase A (MAO-A), and the regulator of G protein signaling (RGS2) (72), 3) miR-196 plays an important regulatory role in schizophrenia (73), 4) miR-132 regulates neurite outgrowth and dendritic morphogenesis (74-76), 5) miR-16 acts as a central effector in 5-HT transporter regulation, mediating the adaptive response of serotonergic and noradrenergic neurons to SSRI antidepressant treatment (77), 6) miR-7 expression is altered in the prefrontal cortex of schizophrenia patients (71), 7) miR-429 is downregulated in response to repeated shocks in a rodent model (78), and 8) miR-107 associated with accelerated disease progression in Alzheimer's disease through regulation of BACE1 ( $\beta$ -site amyloid precursor protein-cleaving enzyme 1) (79).

Still, in our study, the most promising miRNA candidate for diagnostic biomarker was hsa-miR-122, with a 350% decrease in MDD cases at  $p < 0.00004$ . Hsa-miR-122 is highly expressed in the hippocampus (80) and has been implicated in regulation of fatty acid metabolism (81, 82) and circadian rhythm (83). Unfortunately, its role in the central nervous system has not been well established, and understanding its function in the brain requires further studies.

In summary, we believe that a combined miRNA-mRNA analysis approach has a potential to uncover reliable, disease-related panels of biomarkers. The mRNA/miRNA

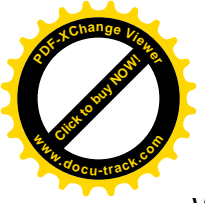


panel identified in this study represents a promising lead, but it will have to be further validated on a different cohort of patients and across different experimental manipulations. Even though in our data sets we did not observe an association between expression and body mass index recorded at the time of the material harvest, we cannot exclude the possibility that some of the observed mRNA/miRNA changes might be related to confounding factors such as life style.

We wish to emphasize that dermal fibroblasts are an appealing experimental model. First, they are easy to obtain and propagate. Second, they are not genetically modified and/or immortalized, yet, the resource is not easily depleted. Third, due to their division in the cell culture, many confounds and epigenetic changes disappear over time. Fourth, our current and previous data suggests that the miRNA and mRNA expression profiles of the fibroblasts from MDD patients are likely to be related to the changes that occur in the brain (25, 30, 84, 85). Fifth, this model is potentially well-suited for *in vitro* drug screening. Finally, establishing this patient-derived model requires only minimal technical and financial resources, and is ideally suited for smaller laboratories. In addition, should the need arise in follow-up experiments, patient fibroblasts can be transformed into iPSCs that can be differentiated into neuronal lineages (86).

### **Acknowledgments:**

KM's work is supported by NIMH grants R01MH067234 and R01 MH079299. RCS work was supported by NIMH grants MH01741, MH52339, and MH073630, and a grant from the Brain & Behavior Research Foundation. We are especially grateful to



Weining Xu, Senior Manager at Qiagen, for her invaluable guidance in the use of the miRNome arrays, and the Vantage Molecular Biology Core at Vanderbilt for their help in carrying out the microarray and miRNome array studies.

**Financial Disclosures:**

KAG, AV, SK, WDT, ZK, GF, JAB and KM have no financial disclosures related to the performed studies. RCS receives unrelated research support from Appian Labs, Assurex, Inc., Cerecor, Inc., Elan, Corp., Euthymics Bioscience, Forest Pharmaceuticals, Janssen Pharmaceutica, Jazz Pharmaceuticals, Naurex, Inc., Novartis Pharmaceuticals, Otsuka Pharmaceuticals, PamLab, Inc., Pfizer, Inc., Repligen, Corp., Ridge Diagnostics, Shire Plc, St. Jude Medical, Inc., Takeda Pharmaceuticals and consults for Bristol-Myers Squibb Company, Cerecor, Inc., Cyberonics, Inc., Eli Lilly and Company, Forest Pharmaceuticals, Janssen Pharmaceutica, Medtronic, Inc., Otsuka Pharmaceuticals, PamLab, Inc., Pfizer, Inc., Ridge Diagnostics, Shire Plc, and Takeda Pharmaceuticals.



## TABLES:

**Table 1. BioCarta GSEA Enrichment of mRNA expression.**

**Table 2. Regulated miRNAs in MDD and their target mRNAs.**

## FIGURE LEGENDS:

**Figure 1. mRNA expression of HGF/MET signaling pathway genes is different between the fibroblasts originating from MDD and CNTRL subjects.**

Y-axis depicts differentially expressed HGF/MET pathway transcripts as defined by BioCarta/GSEA. X-axis denotes Average Log<sub>2</sub> Ratio (ALR) between the MDD and CNTR samples. Bars denote magnitude of change. Note that the vast majority of the genes within this pathway were underexpressed in the MDD fibroblasts.

**Figure 2. Clustering of miRNAs that are differentially expressed between the MDD and CNTR samples.**

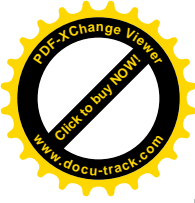
miRNA levels were assessed in 8 pooled samples (4 CNTR + 4 MDD) using miRNome PCR Arrays. 38 miRNAs reported differential expression between fibroblasts from MDD patients and healthy controls. Unsupervised two-way hierarchical clustering of these miRNA expression levels provided a clear separation between the MDD and CNTR samples. Samples were clustered vertically, miRNAs were clustered horizontally. Each colored square represents a normalized miRNA expression level, color coded for increase (red) or decrease (blue) from the mean. Color intensity is proportional to magnitude of change. The clustering resulted in a separation of the samples into two groups, perfectly matching the two distinct diagnostic categories (vertical dendrogram:



green - CNTR samples, purple – MDD samples). For more detail, see **Supplemental Material 4**.

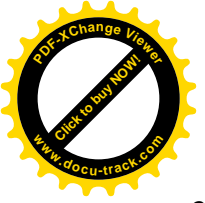
**Figure 3. Differential miRNA expression in pooled MDD fibroblast samples validated on individual samples.**

The expression levels of 7 miRNAs in pooled samples determined by miRNome arrays were validated on individual samples using custom qPCR arrays (n=32, 16 MDD + 16 CNTR).  $\Delta\Delta Ct$  from the pooled samples are plotted on the x-axis,  $\Delta\Delta Ct$ s from individual samples are denoted on the y-axis. Individual data points indicate the expression of 7 miRNA species. Note that the two datasets were highly correlated ( $R^2=0.93$ ,  $p<0.001$ ).



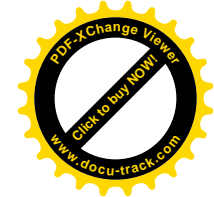
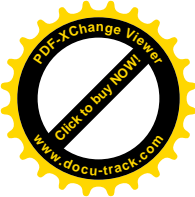
## REFERENCES:

1. Schlaak JF, Trippler M, Hoyo-Becerra C, Erim Y, Kis B, Wang B, et al. (2012): Selective hyper-responsiveness of the interferon system in major depressive disorders and depression induced by interferon therapy. *PLoS One*. 7:e38668.
2. Hepgul N, Cattaneo A, Zunszain PA, Pariante CM (2013): Depression pathogenesis and treatment: what can we learn from blood mRNA expression? *BMC Med*. 11:28.
3. Myint AM (2012): Kynurenines: from the perspective of major psychiatric disorders. *FEBS J*. 279:1375-1385.
4. Chung CP, Schmidt D, Stein CM, Morrow JD, Salomon RM (2012): Increased oxidative stress in patients with depression and its relationship to treatment. *Psychiatry Res*. 206:213-216.
5. Suri R, Helleman G, Cohen L, Aquino A, Altshuler L (2008): Saliva estriol levels in women with and without prenatal antidepressant treatment. *Biol Psychiatry*. 64:533-537.
6. Raedler TJ (2011): Inflammatory mechanisms in major depressive disorder. *Curr Opin Psychiatry*. 24:519-525.
7. Craddock N, Sklar P (2013): Genetics of bipolar disorder. *Lancet*. 381:1654-1662.
8. Israel MA, Yuan SH, Bardy C, Reyna SM, Mu Y, Herrera C, et al. (2012): Probing sporadic and familial Alzheimer's disease using induced pluripotent stem cells. *Nature*. 482:216-220.
9. Hrvoj-Mihic B, Marchetto MC, Gage FH, Semendeferi K, Muotri AR (2013): Novel Tools, Classic Techniques: Evolutionary Studies Using Primate Pluripotent Stem Cells. *Biol Psychiatry*.
10. Shcheglovitov A, Shcheglovitova O, Yazawa M, Portmann T, Shu R, Sebastiano V, et al. (2013): SHANK3 and IGF1 restore synaptic deficits in neurons from 22q13 deletion syndrome patients. *Nature*.
11. Horvath S, Mirnics K (2013): Immune System Disturbances in Schizophrenia. *Biol Psychiatry*.
12. Shelton RC, Claiborne J, Sidoryk-Wegrzynowicz M, Reddy R, Aschner M, Lewis DA, et al. (2010): Altered expression of genes involved in inflammation and apoptosis in frontal cortex in major depression. *Mol Psychiatry*. 16:751-762.
13. Sibille E, Wang Y, Joeyen-Waldorf J, Gaiteri C, Surget A, Oh S, et al. (2009): A molecular signature of depression in the amygdala. *Am J Psychiatry*. 166:1011-1024.
14. Tochigi M, Iwamoto K, Bundo M, Sasaki T, Kato N, Kato T (2008): Gene expression profiling of major depression and suicide in the prefrontal cortex of postmortem brains. *Neurosci Res*. 60:184-191.
15. Kang HJ, Adams DH, Simen A, Simen BB, Rajkowska G, Stockmeier CA, et al. (2007): Gene expression profiling in postmortem prefrontal cortex of major depressive disorder. *J Neurosci*. 27:13329-13340.
16. Evans SJ, Choudary PV, Neal CR, Li JZ, Vawter MP, Tomita H, et al. (2004): Dysregulation of the fibroblast growth factor system in major depression. *Proc Natl Acad Sci U S A*. 101:15506-15511.
17. Edgar N, Sibille E (2012): A putative functional role for oligodendrocytes in mood regulation. *Transl Psychiatry*. 2:e109.
18. Dwivedi Y (2011): Evidence demonstrating role of microRNAs in the etiopathology of major depression. *J Chem Neuroanat*. 42:142-156.
19. Smalheiser NR, Lugli G, Rizavi HS, Torvik VI, Turecki G, Dwivedi Y (2012): MicroRNA expression is down-regulated and reorganized in prefrontal cortex of depressed suicide subjects. *PLoS One*. 7:e33201.
20. Schmidt HD, Shelton RC, Duman RS (2011): Functional biomarkers of depression: diagnosis, treatment, and pathophysiology. *Neuropsychopharmacology*. 36:2375-2394.

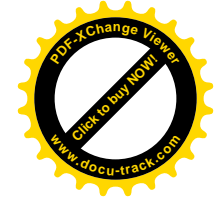
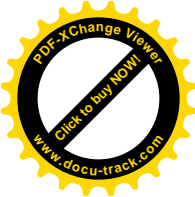


21. Nemeroff CB, Goldschmidt-Clermont PJ (2012): Heartache and heartbreak--the link between depression and cardiovascular disease. *Nat Rev Cardiol.* 9:526-539.
22. Miller AH, Maletic V, Raison CL (2009): Inflammation and its discontents: the role of cytokines in the pathophysiology of major depression. *Biol Psychiatry.* 65:732-741.
23. Belzeaux R, Bergon A, Jeanjean V, Loriod B, Formisano-Treziny C, Verrier L, et al. (2012): Responder and nonresponder patients exhibit different peripheral transcriptional signatures during major depressive episode. *Transl Psychiatry.* 2:e185.
24. Manier DH, Shelton RC, Ellis TC, Peterson CS, Eiring A, Sulser F (2000): Human fibroblasts as a relevant model to study signal transduction in affective disorders. *J Affect Disord.* 61:51-58.
25. Gibson SA, Korade Z, Shelton RC (2012): Oxidative stress and glutathione response in tissue cultures from persons with major depression. *J Psychiatr Res.* 46:1326-1332.
26. Kalman S, Garbett KA, Vereczkei A, Shelton RC, Korade Z, Mirnics K (2013): Metabolic stress-induced microRNA and mRNA expression profiles of human fibroblasts *Exp Cell Res.* in press.
27. Scapagnini G, Davinelli S, Drago F, De Lorenzo A, Oriani G (2012): Antioxidants as antidepressants: fact or fiction? *CNS Drugs.* 26:477-490.
28. Lopresti AL, Maker GL, Hood SD, Drummond PD (2013): A review of peripheral biomarkers in major depression: The potential of inflammatory and oxidative stress biomarkers. *Prog Neuropsychopharmacol Biol Psychiatry.* 48C:102-111.
29. First MB, Pincus HA (2002): The DSM-IV Text Revision: rationale and potential impact on clinical practice. *Psychiatr Serv.* 53:288-292.
30. Akin D, Manier DH, Sanders-Bush E, Shelton RC (2004): Decreased serotonin 5-HT<sub>2A</sub> receptor-stimulated phosphoinositide signaling in fibroblasts from melancholic depressed patients. *Neuropsychopharmacology.* 29:2081-2087.
31. Irizarry RA, Hobbs B, Collin F, Beazer-Barclay YD, Antonellis KJ, Scherf U, et al. (2003): Exploration, normalization, and summaries of high density oligonucleotide array probe level data. *Biostatistics.* 4:249-264.
32. Lazarov O, Robinson J, Tang YP, Hairston IS, Korade-Mirnics Z, Lee VM, et al. (2005): Environmental enrichment reduces Aβ levels and amyloid deposition in transgenic mice. *Cell.* 120:701-713.
33. Unger T, Korade Z, Lazarov O, Terrano D, Schor NF, Sisodia SS, et al. (2005): Transcriptome differences between the frontal cortex and hippocampus of wild-type and humanized presenilin-1 transgenic mice. *Am J Geriatr Psychiatry.* 13:1041-1051.
34. Unger T, Korade Z, Lazarov O, Terrano D, Sisodia SS, Mirnics K (2005): True and false discovery in DNA microarray experiments: transcriptome changes in the hippocampus of presenilin 1 mutant mice. *Methods.* 37:261-273.
35. Arion D, Unger T, Lewis DA, Levitt P, Mirnics K (2007): Molecular evidence for increased expression of genes related to immune and chaperone function in the prefrontal cortex in schizophrenia. *Biol Psychiatry.* 62:711-721.
36. Glorioso C, Sabatini M, Unger T, Hashimoto T, Monteggia LM, Lewis DA, et al. (2006): Specificity and timing of neocortical transcriptome changes in response to BDNF gene ablation during embryogenesis or adulthood. *Mol Psychiatry.* 11:633-648.
37. Kuehn H, Liberzon A, Reich M, Mesirov JP (2008): Using GenePattern for gene expression analysis. *Curr Protoc Bioinformatics.* Chapter 7:Unit 7 12.
38. Subramanian A, Kuehn H, Gould J, Tamayo P, Mesirov JP (2007): GSEA-P: a desktop application for Gene Set Enrichment Analysis. *Bioinformatics.* 23:3251-3253.
39. Khoury H, Naujokas MA, Zuo D, Sangwan V, Frigault MM, Petkiewicz S, et al. (2005): HGF converts ErbB2/Neu epithelial morphogenesis to cell invasion. *Mol Biol Cell.* 16:550-561.

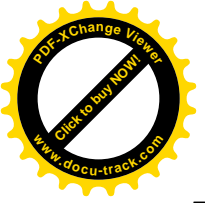




40. O'Carroll D, Schaefer A (2012): General principals of miRNA biogenesis and regulation in the brain. *Neuropsychopharmacology*. 38:39-54.
41. Wang X, El Naqa IM (2008): Prediction of both conserved and nonconserved microRNA targets in animals. *Bioinformatics*. 24:325-332.
42. Wang X (2008): miRDB: a microRNA target prediction and functional annotation database with a wiki interface. *RNA*. 14:1012-1017.
43. Friedman RC, Farh KK, Burge CB, Bartel DP (2009): Most mammalian mRNAs are conserved targets of microRNAs. *Genome Res*. 19:92-105.
44. Carrington JC, Ambros V (2003): Role of microRNAs in plant and animal development. *Science*. 301:336-338.
45. Zhang N, Lin JK, Chen J, Liu XF, Liu JL, Luo HS, et al. (2013): MicroRNA 375 mediates the signaling pathway of corticotropin-releasing factor (CRF) regulating pro-opiomelanocortin (POMC) expression by targeting mitogen-activated protein kinase 8. *J Biol Chem*. 288:10361-10373.
46. Maes M, Yirmiya R, Noraberg J, Brene S, Hibbeln J, Perini G, et al. (2009): The inflammatory & neurodegenerative (I&ND) hypothesis of depression: leads for future research and new drug developments in depression. *Metab Brain Dis*. 24:27-53.
47. Hoffmann A, Spengler D (2012): DNA memories of early social life. *Neuroscience*.
48. Stringer JM, Barrand S, Western P (2013): Fine-tuning evolution: germ-line epigenetics and inheritance. *Reproduction*. 146:R37-48.
49. Organ SL, Tsao MS (2011): An overview of the c-MET signaling pathway. *Ther Adv Med Oncol*. 3:S7-S19.
50. Maina F, Klein R (1999): Hepatocyte growth factor, a versatile signal for developing neurons. *Nat Neurosci*. 2:213-217.
51. van der Voort R, Taher TE, Derksen PW, Spaargaren M, van der Neut R, Pals ST (2000): The hepatocyte growth factor/Met pathway in development, tumorigenesis, and B-cell differentiation. *Adv Cancer Res*. 79:39-90.
52. Arnold SE, Xie SX, Leung YY, Wang LS, Kling MA, Han X, et al. (2012): Plasma biomarkers of depressive symptoms in older adults. *Transl Psychiatry*. 2:e65.
53. Nakaguchi K, Jinnou H, Kaneko N, Sawada M, Hikita T, Saitoh S, et al. (2012): Growth factors released from gelatin hydrogel microspheres increase new neurons in the adult mouse brain. *Stem Cells Int*. 2012:915160.
54. Tanti A, Belzung C (2013): Neurogenesis along the septo-temporal axis of the hippocampus: are depression and the action of antidepressants region-specific? *Neuroscience*. 252:234-252.
55. Raison CL, Capuron L, Miller AH (2006): Cytokines sing the blues: inflammation and the pathogenesis of depression. *Trends Immunol*. 27:24-31.
56. Raison CL, Miller AH (2011): Is depression an inflammatory disorder? *Curr Psychiatry Rep*. 13:467-475.
57. Licinio J, Frost P (2000): The neuroimmune-endocrine axis: pathophysiological implications for the central nervous system cytokines and hypothalamus-pituitary-adrenal hormone dynamics. *Braz J Med Biol Res*. 33:1141-1148.
58. Pandey GN, Rizavi HS, Ren X, Fareed J, Hoppensteadt DA, Roberts RC, et al. (2011): Proinflammatory cytokines in the prefrontal cortex of teenage suicide victims. *J Psychiatr Res*. 46:57-63.
59. Galfalvy H, Zalsman G, Huang YY, Murphy L, Rosoklija G, Dwork AJ, et al. (2011): A pilot genome wide association and gene expression array study of suicide with and without major depression. *World J Biol Psychiatry*.
60. Ripke S, Wray NR, Lewis CM, Hamilton SP, Weissman MM, Breen G, et al. (2012): A mega-analysis of genome-wide association studies for major depressive disorder. *Mol Psychiatry*. 18:497-511.



61. Song GG, Kim JH, Lee YH (2013): Genome-wide pathway analysis in major depressive disorder. *J Mol Neurosci.* 51:428-436.
62. Jia P, Kao CF, Kuo PH, Zhao Z (2012): A comprehensive network and pathway analysis of candidate genes in major depressive disorder. *BMC Syst Biol.* 5 Suppl 3:S12.
63. Su S, Miller AH, Snieder H, Bremner JD, Ritchie J, Maisano C, et al. (2009): Common genetic contributions to depressive symptoms and inflammatory markers in middle-aged men: the Twins Heart Study. *Psychosom Med.* 71:152-158.
64. Wong ML, Dong C, Maestre-Mesa J, Licinio J (2008): Polymorphisms in inflammation-related genes are associated with susceptibility to major depression and antidepressant response. *Mol Psychiatry.* 13:800-812.
65. Wong ML, Dong C, Andreev V, Arcos-Burgos M, Licinio J (2012): Prediction of susceptibility to major depression by a model of interactions of multiple functional genetic variants and environmental factors. *Mol Psychiatry.* 17:624-633.
66. Serafini G, Pompili M, Hansen KF, Obrietan K, Dwivedi Y, Shomron N, et al. (2013): The Involvement of MicroRNAs in Major Depression, Suicidal Behavior, and Related Disorders: A Focus on miR-185 and miR-491-3p. *Cell Mol Neurobiol.*
67. Oved K, Morag A, Pasmanik-Chor M, Oron-Karni V, Shomron N, Rehavi M, et al. (2012): Genome-wide miRNA expression profiling of human lymphoblastoid cell lines identifies tentative SSRI antidepressant response biomarkers. *Pharmacogenomics.* 13:1129-1139.
68. Mouillet-Richard S, Baudry A, Launay JM, Kellermann O (2012): MicroRNAs and depression. *Neurobiol Dis.* 46:272-278.
69. Xu Y, Liu H, Li F, Sun N, Ren Y, Liu Z, et al. (2010): A polymorphism in the microRNA-30e precursor associated with major depressive disorder risk and P300 waveform. *J Affect Disord.* 127:332-336.
70. Saus E, Soria V, Escaramis G, Vivarelli F, Crespo JM, Kagerbauer B, et al. (2010): Genetic variants and abnormal processing of pre-miR-182, a circadian clock modulator, in major depression patients with late insomnia. *Hum Mol Genet.* 19:4017-4025.
71. Kim AH, Reimers M, Maher B, Williamson V, McMichael O, McClay JL, et al. (2010): MicroRNA expression profiling in the prefrontal cortex of individuals affected with schizophrenia and bipolar disorders. *Schizophr Res.* 124:183-191.
72. Muinos-Gimeno M, Espinosa-Parrilla Y, Guidi M, Kagerbauer B, Sipila T, Maron E, et al. (2011): Human microRNAs miR-22, miR-138-2, miR-148a, and miR-488 are associated with panic disorder and regulate several anxiety candidate genes and related pathways. *Biol Psychiatry.* 69:526-533.
73. Guo AY, Sun J, Jia P, Zhao Z (2010): A novel microRNA and transcription factor mediated regulatory network in schizophrenia. *BMC Syst Biol.* 4:10.
74. Kawashima H, Numakawa T, Kumamaru E, Adachi N, Mizuno H, Ninomiya M, et al. (2010): Glucocorticoid attenuates brain-derived neurotrophic factor-dependent upregulation of glutamate receptors via the suppression of microRNA-132 expression. *Neuroscience.* 165:1301-1311.
75. Vo N, Klein ME, Varlamova O, Keller DM, Yamamoto T, Goodman RH, et al. (2005): A cAMP-response element binding protein-induced microRNA regulates neuronal morphogenesis. *Proc Natl Acad Sci U S A.* 102:16426-16431.
76. Wayman GA, Davare M, Ando H, Fortin D, Varlamova O, Cheng HY, et al. (2008): An activity-regulated microRNA controls dendritic plasticity by down-regulating p250GAP. *Proc Natl Acad Sci U S A.* 105:9093-9098.
77. Baudry A, Mouillet-Richard S, Schneider B, Launay JM, Kellermann O (2010): miR-16 targets the serotonin transporter: a new facet for adaptive responses to antidepressants. *Science.* 329:1537-1541.



78. Smalheiser NR, Lugli G, Rizavi HS, Zhang H, Torvik VI, Pandey GN, et al. (2011): MicroRNA expression in rat brain exposed to repeated inescapable shock: differential alterations in learned helplessness vs. non-learned helplessness. *Int J Neuropsychopharmacol.* 14:1315-1325.
79. Wang WX, Rajeev BW, Stromberg AJ, Ren N, Tang G, Huang Q, et al. (2008): The expression of microRNA miR-107 decreases early in Alzheimer's disease and may accelerate disease progression through regulation of beta-site amyloid precursor protein-cleaving enzyme 1. *J Neurosci.* 28:1213-1223.
80. Deng X, Zhong Y, Gu L, Shen W, Guo J (2013): MiR-21 involve in ERK-mediated upregulation of MMP9 in the rat hippocampus following cerebral ischemia. *Brain Res Bull.* 94:56-62.
81. Lagos-Quintana M, Rauhut R, Yalcin A, Meyer J, Lendeckel W, Tuschl T (2002): Identification of tissue-specific microRNAs from mouse. *Curr Biol.* 12:735-739.
82. Lynn FC (2009): Meta-regulation: microRNA regulation of glucose and lipid metabolism. *Trends Endocrinol Metab.* 20:452-459.
83. Gatfield D, Le Martelot G, Vejnar CE, Gerlach D, Schaad O, Fleury-Olela F, et al. (2009): Integration of microRNA miR-122 in hepatic circadian gene expression. *Genes Dev.* 23:1313-1326.
84. Akin D, Manier DH, Sanders-Bush E, Shelton RC (2005): Signal transduction abnormalities in melancholic depression. *Int J Neuropsychopharmacol.* 8:5-16.
85. Shelton RC, Mainer DH, Sulser F (1996): cAMP-dependent protein kinase activity in major depression. *Am J Psychiatry.* 153:1037-1042.
86. Fink KD, Crane AT, Leveque X, Dues DJ, Huffman LD, Moore AC, et al. (2014): Intraatrial Transplantation of Adenovirus-Generated Induced Pluripotent Stem Cells for Treating Neuropathological and Functional Deficits in a Rodent Model of Huntington's Disease. *Stem Cells Transl Med.*



**Table 1. BioCarta GSEA Enrichment of mRNA expression**

#	PATHWAY NAME	SIZE	NES	p-val	Direction
1	AKT: AKT Signaling Pathway	22	-1.61	0.0184	down in MDD
2	CLASSIC: Classical Complement Pathway	12	-1.49	0.0255	
3	ARF: Tumor Suppressor Arf Inhibits Ribosomal Biogenesis	17	-1.55	0.0438	
4	COMP: Complement Pathway	17	-1.42	0.0471	
5	ASBCELL: Antigen Dependent B Cell Activation	12	1.49	0.0061	up in MDD
6	CSK: Activation of Csk by PKA	22	1.51	0.0125	
7	TCR Activation by Lck and Fyn tyrosine kinases	11	1.43	0.0331	
8	TCAPOPTOSIS: HIV Induced T Cell Apoptosis	9	1.53	0.0361	
9	CTLA4: Co-Stimulatory Signal During T-cell Activation	19	1.44	0.0370	
10	NKT: Selective expression of chemokine receptors	28	1.52	0.0385	

miRNA ID	$\Delta\Delta Ct$	<i>p</i> -value	mRNA targets	mRNA up in MDD	mRNA down in MDD	mRNAs up	mRNAs down
hsa-miR-122	2.17	0.0000	157	---	OCLN, MASP1, KCNJ2	0	3
hsa-miR-32	2.01	0.0214	431	BCL11A	LSAMP, CHM, KLF4, SVIP, SSFA2, XPNPEP3, FNIP1, AFF1	1	8
hsa-miR-196b*	1.96	0.0281	16	---	---	0	0
hsa-miR-377	1.62	0.0104	145	---	PTGFR	0	1
hsa-miR-193a-3p	1.52	0.0176	181	HLA-DPB1	DNAJC13, KCNJ2	1	2
hsa-miR-337-5p	1.52	0.0043	27	---	ERAP1	0	1
hsa-miR-675*	1.46	0.0065	185	---	---	0	0
hsa-miR-3176	1.39	0.0172	228	RUFY2	RAC2	1	1
hsa-miR-21*	0.91	0.0396	446	B3GNT7	IL6ST, LSAMP, BMP6	1	3
hsa-miR-22	0.76	0.0423	294	RUFY2	FMNL2, PTGFR, CBL, OGN	1	4
hsa-miR-425*	0.71	0.0227	25	---	---	0	0
hsa-miR-185	0.60	0.0038	430	TRIM58	FAIM2, LSAMP, CPT1A	1	3
hsa-miR-296-5p	0.56	0.0187	111	---	KAZALD1	0	1
hsa-miR-103a	0.55	0.0198	434	BCL11A	PIK3R1, DCLK1, ZCCHC2, MASP1	1	4
hsa-miR-107	0.53	0.0357	452	BCL11A	PIK3R1, DCLK1, ZCCHC2	1	3
hsa-miR-186	0.53	0.0343	1443	FRMD4A	IL6ST, ATP7A, PABPC4L, FNIP1, OCLN, KIAA1324L, AFF1, SFRS6, MET	1	9
hsa-miR-887	0.45	0.0277	22	---	---	0	0

**LEGEND:** Red - upregulated mRNAs in MDD; Green - downregulated mRNAs in MDD; Bold symbols - regulated by multiple miRNAs

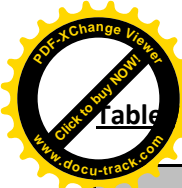
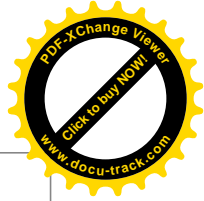
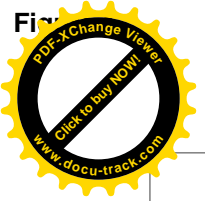


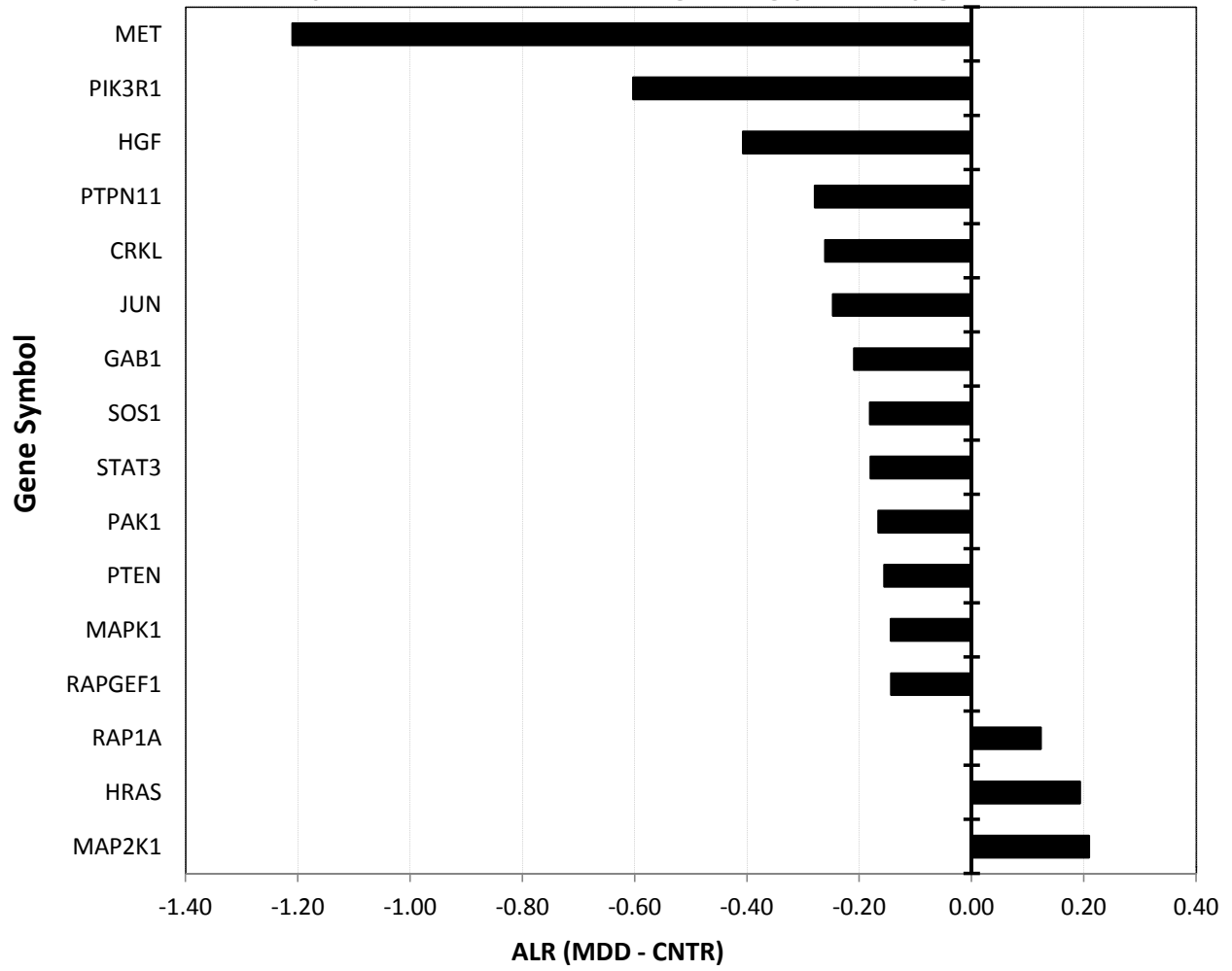
**Table 2. Upregulated miRNAs in MDD and their putative mRNA expression targets**

miRNA ID	$\Delta\Delta Ct$	<i>p</i> -value	mRNA targets	mRNA up in MDD	mRNA down in MDD	mRNAs up	mRNAs down
hsa-mir-132	-0.42	0.0028	537	<b>SLC2A1</b>	ANKRD29, ENPP4, PCDH10	1	3
hsa-mir-421	-0.43	0.0013	468	<b>SCG2</b>	BMP2, RASSF8, PTGFR, PTGES	1	4
hsa-mir-542	-0.44	0.0078	209		KIAA1324L	0	1
hsa-mir-450a	-0.50	0.0233	20	---	---	0	0
hsa-mir-16-2* (3p)	-0.54	0.0381	868	<b>MSTN, RUFY2</b>	PIK3R1, FMNL2, ATP7A, DDIT4L, PABPC4L, ERAP1, OGN, MET	2	8
hsa-mir-424	-0.69	0.0309	885		PIK3R1, HSPA4L, ZFH4, MLL3, DCLK1, ATP7A, RASSF8, SVEP1, ENPP4, ZCCHC2, MASP1, KCNJ2	0	12
hsa-mir-628-3p	-0.72	0.0101	231	---	AMPD3	0	1
hsa-mir-629-5p	-0.76	0.0244	224	---	NFIB	0	1
hsa-mir-4293	-0.77	0.0086	234	---	PTGFR	0	1
hsa-mir-661	-0.80	0.0072	315	<b>B3GNT7</b>	PCDH10	1	1
hsa-mir-3909	-0.80	0.0286	178	<b>HLA-DRA</b>	CHM, PTGFRN, PDE1A	1	3
hsa-mir-33a* (3p)	-0.80	0.0156	1541	<b>MSTN, LEF1</b>	SEMA3D, CCNL1, RALGPS2, DCLK1, HECTD1, EHBP1, EIF4G3, AHNAK, ETV1, RASSF8, PTGFR, DDIT4L, KIAA1324L, ERAP1, TNFRSF19, AFF1, OGN	2	17
hsa-mir-135b	-0.84	0.0289	405	---	IGF2BP3, KLF4, IL1R1, PABPC4L, IGF2BP3	0	5
hsa-mir-7	-0.96	0.0320	675	<b>TRIM58</b>	KLF4, CBL, KCNJ2	1	3
hsa-mir-4267	-0.97	0.0360	272	---	PREX1, SSFA2, XPNPEP3, AFF1	0	4
hsa-mir-548a-3p	-1.05	0.0052	1118	---	PIK3R1, IGF2BP3, CYP1B1, ZFH4, RAPGEF2, IL1R1, SSFA2, CBL, OCLN, PDE1A, IGF2BP3, DDX17	2	12
hsa-mir-548d-3p	-1.25	0.0120	1380	<b>LEF1, SLC2A1</b>	ZBTB38, FOXP2, RALGPS2, MLL3, PER3, DCLK1, ATP7A, IL1R1, XPNPEP3, OCLN	2	10
hsa-mir-613	-1.53	0.0025	371	---	CHM, ANKRD29, PAX3, OGN, MET	1	5
hsa-mir-3714	-1.58	0.0202	545	---	SEMA3D, RALGPS2, ERC1, AMPD3, CPT1A, CBL, PABPC4L, AFF1, KCNJ2, BMP6	0	10
hsa-mir-1294	-1.78	0.0371	165	---	---	0	0
hsa-mir-429	-2.00	0.0109	842	<b>MSTN, FRMD4A</b>	RALGPS2, CHM, KLF4, RAPGEF2, RASSF8, SSFA2, OCLN	2	7

**LEGEND:** Red - upregulated mRNAs in MDD; Green - downregulated mRNAs in MDD; Bold symbols - regulated by multiple miRNAs

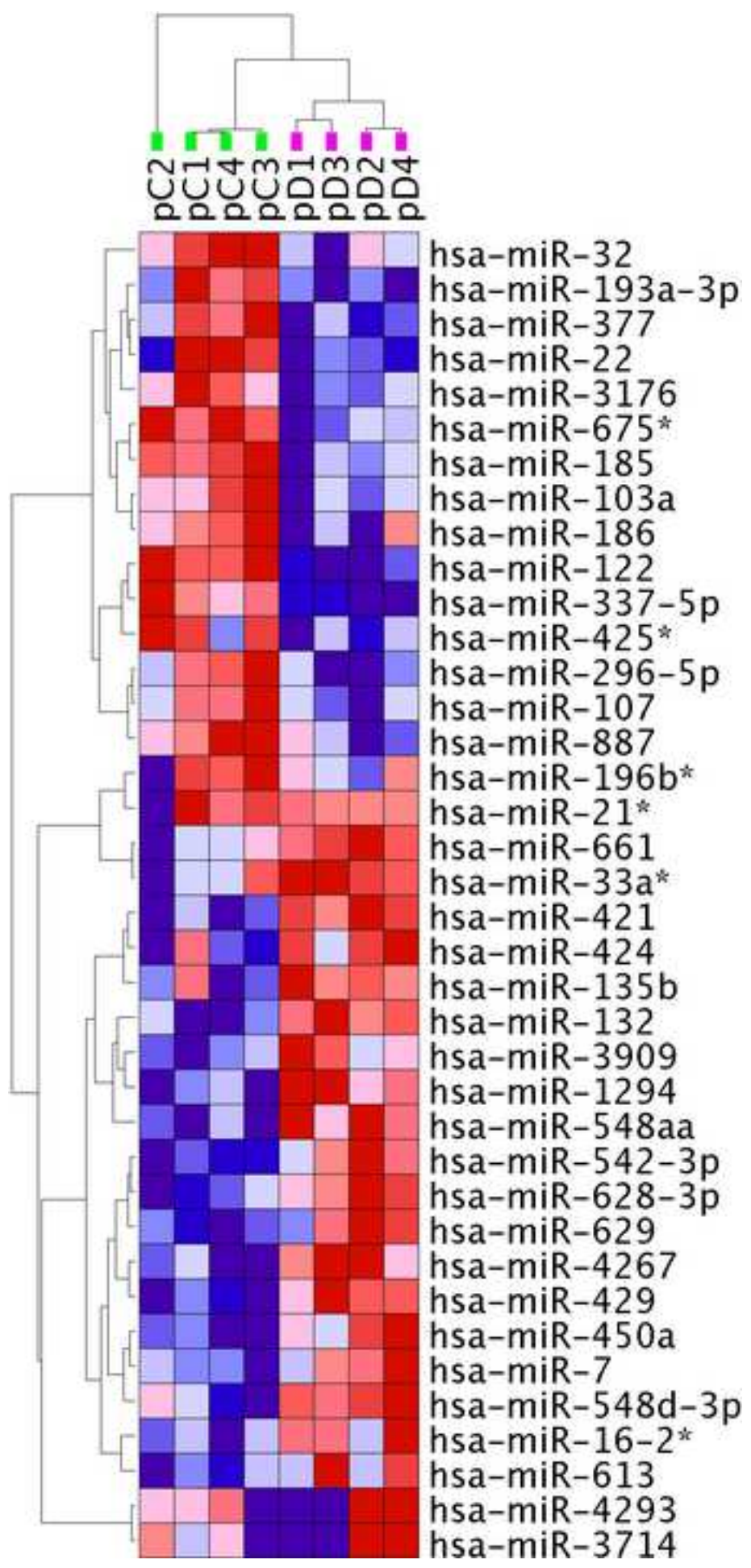
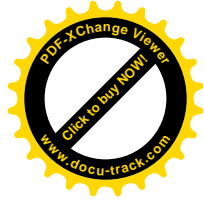


### mRNA expression of HGF/MET signaling pathway genes

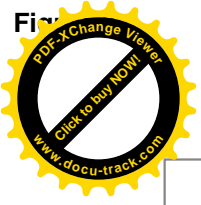




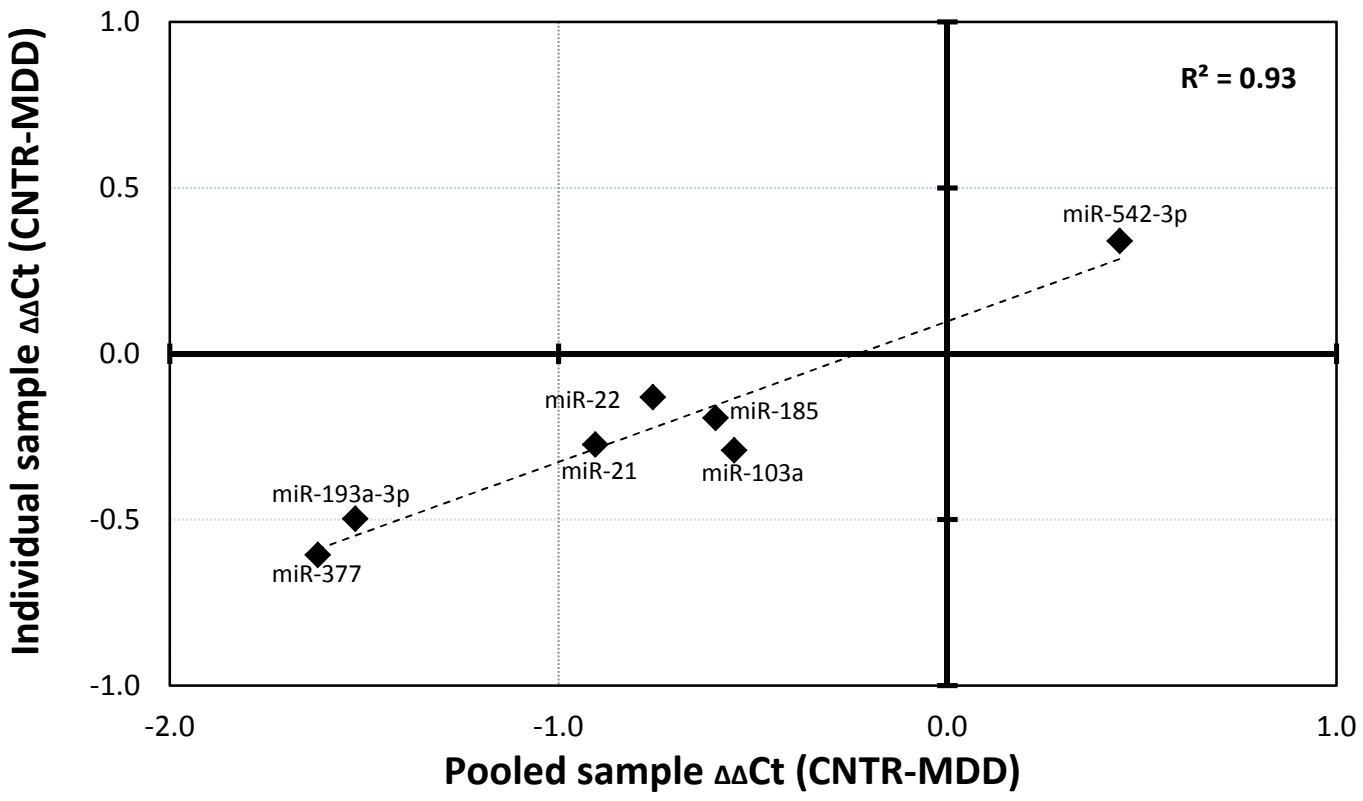
download high resolution image

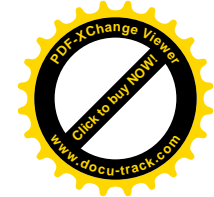






### Correlation of miRNA levels in pooled and individual samples





## SUPPLEMENTAL MATERIAL:

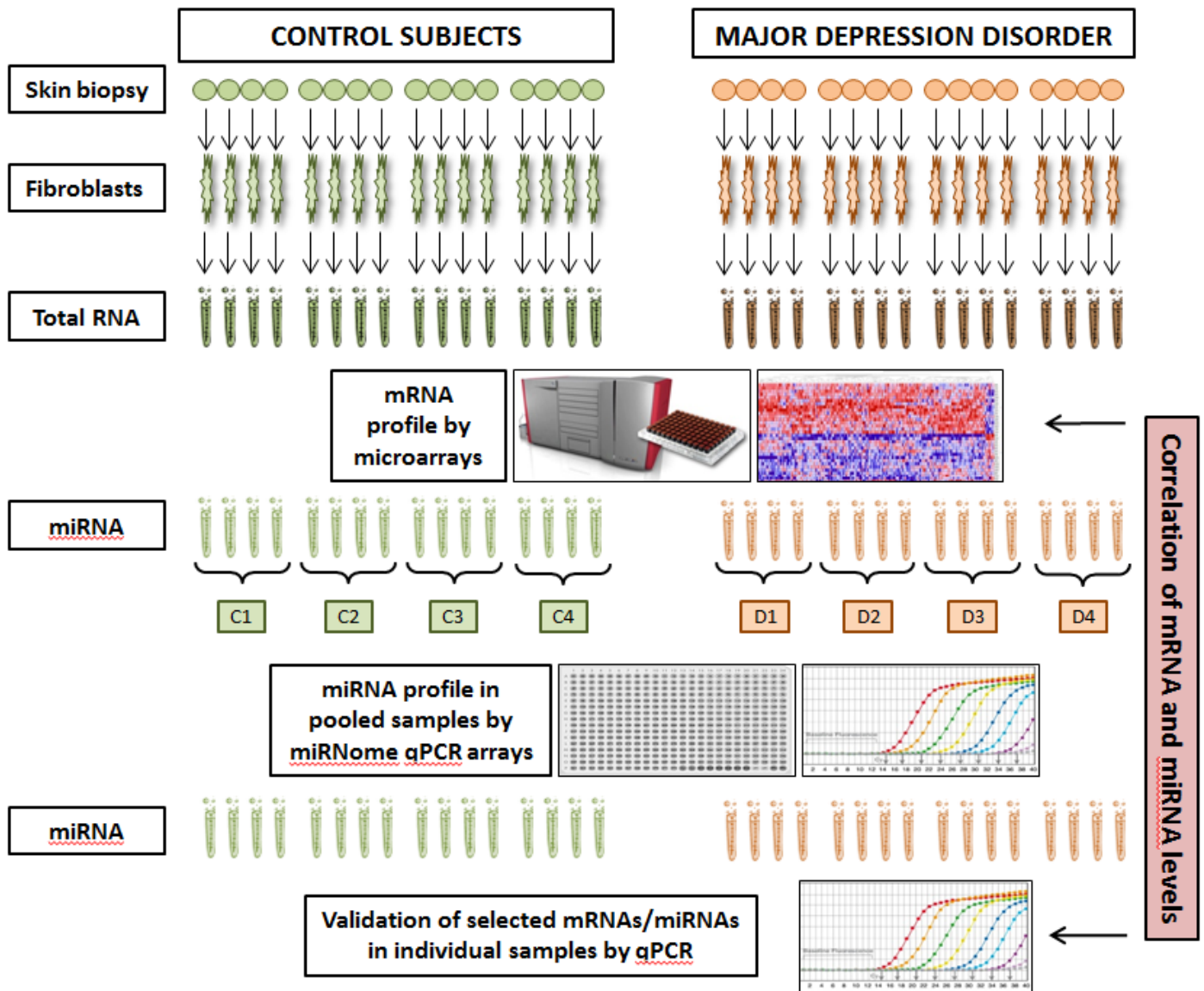
### Supplemental Material 1. Subject information

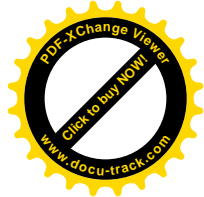
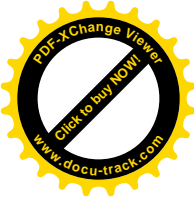
Group	ID	Age	AVG Age	Sex	Race	BMI	Group	ID	Age	AVG Age	Sex	Race	BMI
CNTR1	C1	34	37.5	M	AA	23.1	MDD1	D1	38	36.5	M	AA	31.6
	C2	38		M	W	20.5		D2	33		M	W	41.9
	C3	48		M	W	N/A		D3	46		M	W	31
	C4	30		M	W	N/A		D4	29		M	W	19
CNTR2	C5	35	32.25	F	W	27.1	MDD2	D5	34	31	F	W	N/A
	C6	40		F	W	21.2		D6	37		F	W	N/A
	C7	27		F	W	21.8		D7	27		F	W	46.2
	C8	27		F	AA	34.7		D8	26		F	AA	31.4
CNTR3	C9	51	49	F	AA	26	MDD3	D9	51	49.75	F	AA	28.9
	C10	49		F	W	26.2		D10	52		F	W	24
	C11	52		F	W	26.3		D11	53		F	W	28
	C12	44		F	W	25.1		D12	43		F	W	50.7
CNTR4	C13	20	21.8	F	W	24	MDD4	D13	22	22.4	F	W	49.8
	C14	22		F	W	26.8		D14	22		F	W	22.5
	C15	22		F	W	22		D15	23		F	W	30.1
	C16	25		F	AA	30.5		D16	23		F	AA	18.4

M-male, F-female, AA-African-American, W-white, BMI-body mass index

## Supplemental Material 2. Experimental design

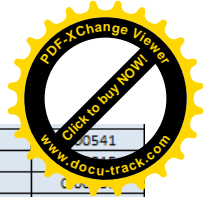
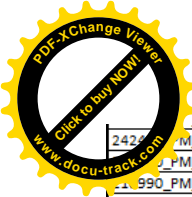
Skin biopsies were obtained using tissue punches from 16 MDD patients and 16 matched control subjects. Fibroblasts were propagated in tissue cultures with matching patient/control pairs cultured simultaneously under same conditions. This was followed by isolation on mRNA and miRNA. Individual mRNA expression profile was determined using GeneChip HT HG-U133+ PM Array Plate (Affymetrix Inc, Santa Clara, CA, USA). Initial miRNA profiling was performed using miRNome miRNA PCR Arrays (Qiagen, Valencia, CA, USA). The individual sample cDNAs were pooled in equal proportions into four groups based on gender and age (**Supplemental Material 1**). The most robustly changed miRNAs were validated using qPCR on individual samples. To better understand the relationship between the mRNA and miRNA changes, we correlated the two datasets based on the predicted miRNA targets.





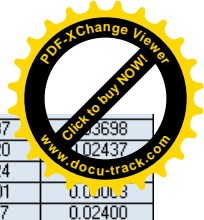
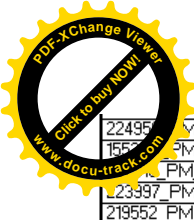
**Supplemental Material 3. mRNA expression changes between fibroblasts originating from MDD patients and matched healthy controls.** CNTR and MDD columns denote average log<sub>2</sub> expression levels for the two diagnostic classes, ALR column represents magnitude of differential expression (positive values denote higher expression in MDD, negative values correspond to higher expression in controls). Paired ttest – pairwise comparison p-value; Group ttest – groupwise comparison p-value. Note that the - downregulated genes in MDD fibroblasts greatly outnumber the upregulated ones.

Probe Set ID	Public ID	Gene Symbol	Gene Name	CNTR	MDD	ALR (MDD-CNTR)	paired ttest	group ttest
208894_PM_at	M60334	HLA-DRA	major histocompatibility complex, class II, DR alpha	5.31	7.17	1.86	0.02893	0.04768
229479_PM_at	AJ739132	---	---	7.11	8.87	1.76	0.01735	0.01206
215193_PM_x_at	AJ297586	HLA-DRB	major histocompatibility complex, class II, DR beta	5.30	7.00	1.70	0.02389	0.04638
210982_PM_s_at	M60333	HLA-DRA	major histocompatibility complex, class II, DR alpha	5.74	7.40	1.66	0.02374	0.04891
209619_PM_at	K01144	CD74	CD74 molecule, major histocompatibility complex, class II invariant chain	5.88	7.39	1.51	0.02547	0.04955
215047_PM_at	AL080170	TRIM58	tripartite motif-containing 58	4.64	5.99	1.34	0.01396	0.01728
204035_PM_at	NM_003469	SCG2	secretogranin II	6.80	8.07	1.27	0.00706	0.01554
201137_PM_s_at	NM_002121	HLA-DPB1	major histocompatibility complex, class II, DP beta 1	6.85	7.99	1.15	0.02463	0.03573
1558882_PM_at	BI868572	LOC401233	cofactor required for Tat activation of HIV-1 transcription	5.60	6.56	0.96	0.00437	0.02345
229802_PM_at	AA147884	---	---	10.46	11.28	0.81	0.03227	0.03040
1555963_PM_x_at	CA503291	B3GN7	UDP-GlcNAc:betaGal beta-1,3-N-acetylglucosaminyltransferase 7	4.21	5.02	0.81	0.02155	0.02074
213831_PM_at	X00452	HLA-DQA1	major histocompatibility complex, class II, DQ alpha 1	4.03	4.83	0.80	0.03874	0.04060
1555962_PM_at	CA503291	B3GN7	UDP-GlcNAc:betaGal beta-1,3-N-acetylglucosaminyltransferase 7	4.25	5.04	0.79	0.01367	0.02526
215014_PM_at	AL512727	KCNDB3	potassium voltage-gated channel, Shal-related subfamily, member 3	6.94	7.69	0.75	0.00954	0.00514
221854_PM_at	AI378979	PKP1	plakophilin 1 (ectodermal dysplasia/skin fragility syndrome)	4.22	4.96	0.74	0.03414	0.04686
211836_PM_s_at	U18800	MOG	myelin oligodendrocyte glycoprotein	4.03	4.73	0.70	0.00588	0.03425
207145_PM_at	NM_005259	MSTN	myostatin	4.62	5.31	0.69	0.04953	0.03888
221558_PM_s_at	AF288571	LEF1	lymphoid enhancer-binding factor 1	4.57	5.25	0.68	0.01958	0.03653
1569942_PM_at	BC037802	---	---	4.11	4.77	0.66	0.01611	0.02984
233337_PM_at	AF131749	SEZ6L2	seizure related 6 homolog (mouse)-like 2	6.18	6.83	0.65	0.01618	0.04045
201250_PM_s_at	NM_006516	SLC2A1	solute carrier family 2 (facilitated glucose transporter), member 1	7.06	7.71	0.64	0.01076	0.02150
206560_PM_s_at	NM_006533	MIA	melanoma inhibitory activity	4.88	5.51	0.63	0.00887	0.03750
1554133_PM_at	BC041092	RUFY2	RUN and FYVE domain containing 2	5.33	5.95	0.62	0.02043	0.02962
1560031_PM_at	R19413	FRMD4A	FERM domain containing 4A	5.61	6.21	0.60	0.03118	0.03774
219497_PM_s_at	NM_022893	BCL11A	B-cell CLL/lymphoma 11A (zinc finger protein)	6.66	7.25	0.59	0.04756	0.02429
230574_PM_at	AW139393	LOC100130938	hypothetical LOC100130938	4.98	5.57	0.59	0.00697	0.00790
231361_PM_at	AI912122	NLGN1	neuroligin 1	7.28	6.70	-0.59	0.03680	0.04543
204864_PM_s_at	NM_002184	IL6ST	interleukin 6 signal transducer (gp130, oncostatin M receptor)	8.18	7.59	-0.59	0.00121	0.00032
211839_PM_s_at	U22386	CSF1	colony stimulating factor 1 (macrophage)	5.78	5.19	-0.59	0.00756	0.00604
219247_PM_s_at	NM_024630	ZDHHC14	zinc finger, DHHC-type containing 14	6.79	6.20	-0.59	0.00009	0.00116
213309_PM_at	AL117515	PLCL2	phospholipase C-like 2	6.93	6.34	-0.59	0.02215	0.01868
212992_PM_at	AI935123	AHNAK2	AHNAK nucleoprotein 2	10.27	9.68	-0.60	0.01680	0.03502
211572_PM_s_at	AF092511	SLC23A2	solute carrier family 23 (nucleobase transporters), member 2	6.41	5.80	-0.60	0.00002	0.00001
212240_PM_s_at	AI679268	PIK3R1	phosphoinositide-3-kinase, regulatory subunit 1 (alpha)	9.38	8.78	-0.60	0.01641	0.00986
220945_PM_x_at	NM_018050	MANSC1	MANSC domain containing 1	6.50	5.90	-0.60	0.02106	0.02263
239002_PM_at	AA748494	ASPM	asp (abnormal spindle) homolog, microcephaly associated	6.01	5.40	-0.60	0.01244	0.00882
1560020_PM_at	BC043583	DNAJC13	DnaJ (Hsp40) homolog, subfamily C, member 13	7.09	6.48	-0.61	0.00051	0.00006
236557_PM_at	AW085625	ZBTB38	zinc finger and BTB domain containing 38	7.78	7.17	-0.61	0.00011	0.00001
214537_PM_at	NM_005320	HIST1H1D	histone cluster 1, H1d	5.73	5.12	-0.61	0.00393	0.00330
215324_PM_at	AA343027	SEMA3D	semaphorin 3D	5.77	5.16	-0.61	0.02033	0.01689
216493_PM_s_at	AL023775	IGF2BP3	insulin-like growth factor 2 mRNA binding protein 3	6.09	5.48	-0.61	0.03735	0.01742
220580_PM_at	NM_025044	BICC1	bicaudal C homolog 1 (Drosophila)	6.83	6.22	-0.61	0.00263	0.00790
205543_PM_at	NM_014278	HSPA4L	heat shock 70kDa protein 4-like	6.52	5.91	-0.61	0.00142	0.01122
203619_PM_s_at	NM_012306	FAIM2	Fas apoptotic inhibitory molecule 2	5.58	4.97	-0.62	0.04341	0.04587
216218_PM_s_at	AK023546	PLCL2	phospholipase C-like 2	5.81	5.19	-0.62	0.00770	0.00090
241495_PM_at	AI675298	CCNL1	cyclin L1	6.08	5.45	-0.62	0.02390	0.01103
242665_PM_at	AL042120	FMNL2	formin-like 2	6.21	5.58	-0.62	0.00541	0.00058
229244_PM_at	AI400057	LSAMP	limbic system-associated membrane protein	5.97	5.34	-0.63	0.01310	0.01848
202434_PM_s_at	N21019	CYP1B1	cytochrome P450, family 1, subfamily B, polypeptide 1	9.77	9.14	-0.63	0.03448	0.01964
227463_PM_at	AW057540	ACE	angiotensin I converting enzyme (peptidyl-dipeptidase A) 1	5.66	5.03	-0.63	0.01802	0.04951
219779_PM_at	NM_024721	ZFXH4	zinc finger homeobox 4	8.39	7.76	-0.63	0.04016	0.02516
235201_PM_at	AW167727	FOXP2	forkhead box P2	8.02	7.39	-0.64	0.04573	0.04479
242458_PM_at	AA721230	RAI1	Rai GFF with PH domain and SH3 binding motif 2	6.92	6.28	-0.64	0.00774	0.00541



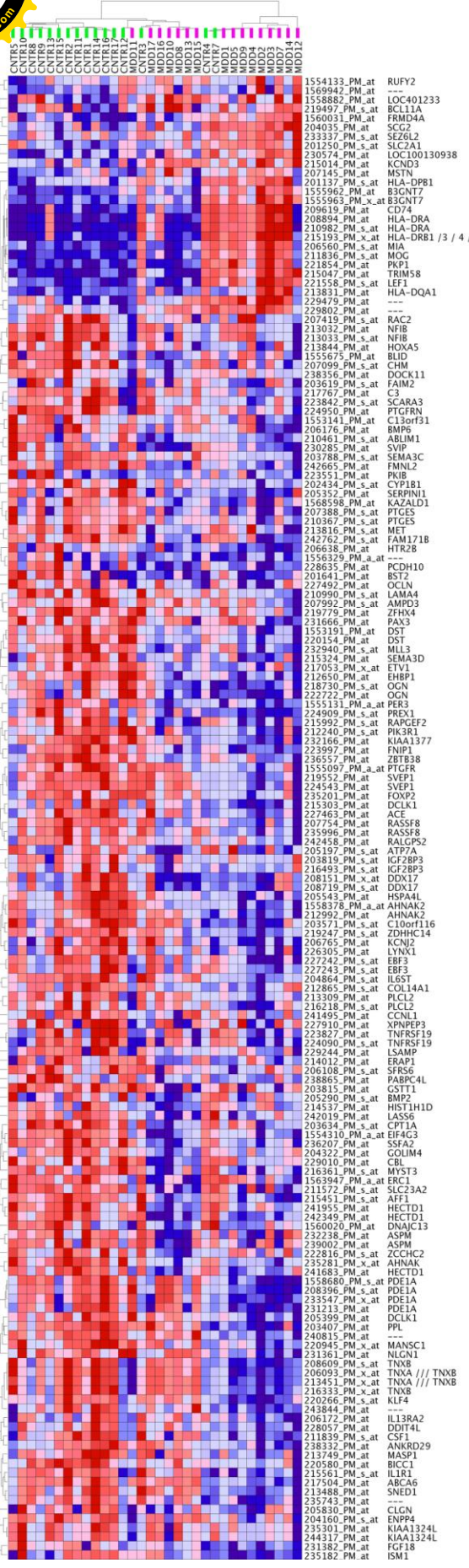
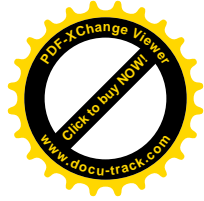
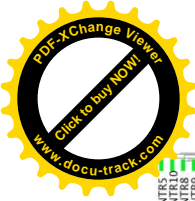
24247_PM_at	AA721230	RALGPS2	Ral GEF with PH domain and SH3 binding motif 2	6.92	6.28	-0.64	0.00774	0.00541
211990_PM_s_at	AK025911	MLL3	myeloid/lymphoid or mixed-lineage leukemia 3	7.22	6.58	-0.64	0.00082	0.00000
220154_PM_at	U77706	LAMA4	laminin, alpha 4	10.44	9.80	-0.64	0.00040	0.00000
220154_PM_at	NM_020388	DST	dystonin	6.21	5.57	-0.64	0.00117	0.00010
1555131_PM_a_at	BC026102	PER3	period homolog 3 (Drosophila)	5.57	4.93	-0.64	0.00102	0.00049
213844_PM_at	NM_019102	HOUA5	homeobox A5	6.19	5.55	-0.64	0.02158	0.01117
207419_PM_s_at	NM_002872	RAC2	ras-related C3 botulinum toxin substrate 2	6.44	5.79	-0.65	0.02733	0.02948
1556329_PM_a_at	BC042378	---	---	4.49	3.85	-0.65	0.04453	0.02951
207099_PM_s_at	NM_000390	CHM	choroideremia (Rab escort protein 1)	7.35	6.71	-0.65	0.00014	0.00000
232238_PM_at	AK001380	ASPM	asp (abnormal spindle) homolog, microcephaly associated	6.63	5.98	-0.65	0.00474	0.00401
215303_PM_at	BE046461	DCLK1	doublecortin-like kinase 1	5.11	4.46	-0.65	0.01074	0.03212
1563947_PM_a_at	AK097177	ERC1	ELKS/RAB6-interacting/CAST family member 1	6.89	6.24	-0.65	0.00000	0.00013
216361_PM_s_at	AJ251844	MYST3	MYST histone acetyltransferase (monocytic leukemia) 3	5.37	4.72	-0.65	0.00007	0.00001
220266_PM_s_at	NM_004235	KLF4	Kruppel-like factor 4 (gut)	8.40	7.74	-0.65	0.01748	0.00618
1555675_PM_at	AF303179	BLID	BH3-like motif containing, cell death inducer	6.01	5.35	-0.66	0.00665	0.00840
205197_PM_s_at	BE567813	ATP7A	ATPase, Cu++ transporting, alpha polypeptide	7.01	6.35	-0.66	0.00119	0.00159
223842_PM_s_at	AB007830	SCARA3	scavenger receptor class A, member 3	7.49	6.83	-0.66	0.01892	0.03511
242019_PM_at	BG257755	LASS6	LAG1 homolog, ceramide synthase 6	5.47	4.80	-0.66	0.00009	0.00010
223551_PM_at	AF225513	PKIB	protein kinase (cAMP-dependent, catalytic) inhibitor beta	4.51	3.84	-0.66	0.02345	0.03252
215992_PM_s_at	AL117397	RAPGEF2	Rap guanine nucleotide exchange factor (GEF) 2	6.48	5.81	-0.67	0.00009	0.00001
242349_PM_at	AW275658	HECTD1	HECT domain containing 1	7.77	7.11	-0.67	0.00000	0.00000
1568598_PM_at	BF434771	KAZALD1	Kazal-type serine peptidase inhibitor domain 1	6.29	5.62	-0.67	0.02721	0.01036
231382_PM_at	AF798863	FGF18	fibroblast growth factor 18	5.40	4.73	-0.67	0.04928	0.03708
224909_PM_s_at	BF308645	PREX1	phosphatidylinositol-3,4,5-trisphosphate-dependent Rac exchange factor 1	5.51	4.84	-0.68	0.00030	0.00016
1553191_PM_at	NM_020388	DST	dystonin	8.06	7.38	-0.68	0.00211	0.00037
205290_PM_s_at	NM_001200	BMP2	bone morphogenetic protein 2	5.25	4.57	-0.68	0.00271	0.00959
212650_PM_at	BF116032	EHBP1	EH domain binding protein 1	10.65	9.97	-0.69	0.00004	0.00004
204322_PM_at	BF002254	GOLIM4	golgi integral membrane protein 4	6.91	6.21	-0.70	0.00001	0.00006
230285_PM_at	BF447829	SVIP	small VCP/p97-interacting protein	5.19	4.49	-0.70	0.00232	0.00231
243844_PM_at	AI816790	---	---	5.51	4.81	-0.70	0.02986	0.03983
203788_PM_s_at	AI962897	SEMA3C	semaphorin 3C	9.95	9.24	-0.70	0.03050	0.01035
232166_PM_at	AL045516	KIAA1377	KIAA1377	7.23	6.52	-0.71	0.00042	0.00105
1554310_PM_a_at	BC030578	EIF4G3	eukaryotic translation initiation factor 4 gamma, 3	7.41	6.70	-0.71	0.00000	0.00000
206638_PM_at	NM_000867	HTR2B	5-hydroxytryptamine (serotonin) receptor 2B	4.52	3.80	-0.72	0.03023	0.02146
217504_PM_at	AA099357	ABCA6	ATP-binding cassette, sub-family A (ABC1), member 6	7.31	6.59	-0.72	0.01175	0.03929
235281_PM_x_at	AA523289	AHNAK	AHNAK nucleoprotein	7.79	7.07	-0.73	0.00000	0.00000
241955_PM_at	BE243270	HECTD1	HECT domain containing 1	8.87	8.15	-0.73	0.00000	0.00001
217053_PM_x_at	X87175	ETV1	ets variant 1	5.80	5.07	-0.73	0.03184	0.00638
215561_PM_s_at	AK026803	IL1R1	interleukin 1 receptor, type I	7.34	6.61	-0.73	0.00837	0.01801
207992_PM_s_at	NM_000480	AMPD3	adenosine monophosphate deaminase 3	7.97	7.23	-0.73	0.01784	0.01575
238356_PM_at	AW968823	DOCK11	dedicator of cytokinesis 11	6.90	6.17	-0.73	0.00793	0.00332
235996_PM_at	BF979984	RASSF8	Ras association (RalGDS/AF-6) domain family (N-terminal) member 8	7.43	6.70	-0.73	0.00147	0.00054
213033_PM_s_at	AI186739	NFIB	nuclear factor I/B	7.26	6.52	-0.74	0.03147	0.02905
210461_PM_s_at	BC002448	ABLIM1	actin binding LIM protein 1	5.96	5.21	-0.75	0.00285	0.00265
236207_PM_at	BE083088	SSFA2	sperm specific antigen 2	6.32	5.57	-0.75	0.00002	0.00000
238332_PM_at	AI307802	ANKRD29	ankyrin repeat domain 29	7.37	6.61	-0.76	0.00697	0.00792
1555097_PM_a_at	BC035694	PTGFR	prostaglandin F receptor (FP)	9.00	8.24	-0.76	0.02465	0.04005
203634_PM_s_at	NM_001876	CPT1A	carnitine palmitoyltransferase 1A (liver)	5.90	5.14	-0.76	0.00000	0.00000
229010_PM_at	AI807026	CBL	Cas-Br-M (murine) ecotropic retroviral transforming sequence	7.67	6.91	-0.76	0.00002	0.00009
231666_PM_at	AA194168	PAX3	paired box 3	6.82	6.06	-0.76	0.04452	0.02876
228057_PM_at	AA528140	DDIT4L	DNA-damage-inducible transcript 4-like	6.20	5.44	-0.76	0.00680	0.01095
238865_PM_at	AI822134	PABPC4L	poly(A) binding protein, cytoplasmic 4-like	6.06	5.30	-0.76	0.03726	0.02234
224543_PM_at	AF308289	SVEP1	sushi, von Willebrand factor type A, EGF and pentraxin domain containing 1	7.39	6.62	-0.77	0.02379	0.03056
224950_PM_at	BF476250	PTGFRN	prostaglandin F2 receptor negative regulator	8.10	7.33	-0.77	0.00887	0.03698

Supplemental Material 3. continued



22495_PM_at	BF476250	PTGFRN	prostaglandin F2 receptor negative regulator	8.10	7.33	-0.77	0.00887	0.03698
15577_PM_at	BC035749	C13orf31	chromosome 13 open reading frame 31	7.53	6.76	-0.77	0.03820	0.02437
22397_PM_at	AI635379	XPNPPEP3	X-prolyl aminopeptidase (aminopeptidase P) 3, putative	6.75	5.97	-0.77	0.00924	0.03345
22397_PM_at	BC001956	FNIP1	folliculin interacting protein 1	6.47	5.69	-0.78	0.00001	0.03003
219552_PM_at	NM_024500	SVEP1	sushi, von Willebrand factor type A, EGF and pentraxin domain co	7.86	7.08	-0.78	0.01237	0.02400
226305_PM_at	AV696976	LYNX1	Ly6/neurotoxin 1	7.12	6.34	-0.78	0.02177	0.03345
204160_PM_s_at	AW194947	ENPP4	ectonucleotide pyrophosphatase/phosphodiesterase 4 (putative fur	7.39	6.60	-0.78	0.00893	0.02243
227492_PM_at	AI829721	OCLN	occludin	6.10	5.30	-0.79	0.04518	0.03142
241683_PM_at	AW207734	HECTD1	HECT domain containing 1	6.19	5.39	-0.80	0.00000	0.00000
242762_PM_s_a	AA372349	FAM171B	family with sequence similarity 171, member B	6.24	5.44	-0.80	0.00028	0.00018
213488_PM_at	N73970	SNED1	sushi, nidogen and EGF-like domains 1	8.90	8.10	-0.80	0.01682	0.02093
222816_PM_s_at	BE676543	ZCCHC2	zinc finger, CCHC domain containing 2	6.94	6.13	-0.81	0.00769	0.00401
235301_PM_at	AI797353	KIAA1324L	KIAA1324-like	8.08	7.26	-0.81	0.04383	0.04483
231213_PM_at	AU146305	PDE1A	phosphodiesterase 1A, calmodulin-dependent	5.08	4.27	-0.81	0.00826	0.03124
244317_PM_at	BF035563	KIAA1324L	KIAA1324-like	7.33	6.51	-0.82	0.02203	0.02105
214012_PM_at	BE551138	ERAP1	endoplasmic reticulum aminopeptidase 1	6.16	5.34	-0.82	0.01352	0.02543
213749_PM_at	AV686235	MASP1	mannan-binding lectin serine peptidase 1	7.07	6.23	-0.84	0.01552	0.01738
223827_PM_at	AF246998	TNFRSF19	tumor necrosis factor receptor superfamily, member 19	6.54	5.70	-0.84	0.04530	0.01480
203819_PM_s_at	AU160004	IGFBP3	insulin-like growth factor 2 mRNA binding protein 3	7.61	6.77	-0.85	0.03655	0.02416
240815_PM_at	R62588	---	---	6.69	5.84	-0.85	0.01266	0.00622
207754_PM_at	NM_007211	RASSF8	Ras association (RalGDS/AF-6) domain family (N-terminal) membe	7.58	6.72	-0.85	0.00008	0.00001
203571_PM_s_at	NM_006829	C10orf116	chromosome 10 open reading frame 116	9.01	8.15	-0.86	0.01469	0.04169
207388_PM_s_a	NM_004878	PTGES	prostaglandin E synthase	7.85	6.99	-0.86	0.03371	0.00913
227243_PM_s_a	AL354950	EBF3	early B-cell factor 3	6.81	5.93	-0.88	0.00248	0.00701
205352_PM_at	NM_005025	SERPIN1	serpin peptidase inhibitor, clade I (neuroserpin), member 1	6.37	5.48	-0.89	0.00626	0.01004
215451_PM_s_at	BF575588	AFF1	AF4/FMR2 family, member 1	6.86	5.95	-0.91	0.00000	0.00000
213032_PM_at	AI86739	NFIB	nuclear factor I/B	8.36	7.43	-0.93	0.04215	0.03556
217767_PM_at	NM_000064	C3	complement component 3	8.05	7.10	-0.95	0.00357	0.01306
201641_PM_at	NM_004335	BST2	bone marrow stromal cell antigen 2	5.22	4.26	-0.96	0.02141	0.00839
235743_PM_at	AA808178	---	---	7.61	6.64	-0.97	0.00972	0.01408
212865_PM_s_at	BF449063	COL14A1	collagen, type XIV, alpha 1	7.88	6.91	-0.97	0.02833	0.03163
206765_PM_at	AF153820	KCNJ2	potassium inwardly-rectifying channel, subfamily J, member 2	6.70	5.72	-0.98	0.02105	0.03535
233547_PM_x_a	N53248	PDE1A	phosphodiesterase 1A, calmodulin-dependent	6.66	5.67	-0.98	0.01056	0.03217
205830_PM_at	NM_004362	CLGN	calmegin	5.70	4.71	-0.99	0.01615	0.01278
224090_PM_s_a	AB040434	TNFRSF19	tumor necrosis factor receptor superfamily, member 19	6.69	5.69	-1.00	0.02977	0.00854
206108_PM_s_at	NM_006275	SFRS6	splicing factor, arginine/serine-rich 6	9.23	8.22	-1.00	0.02418	0.03451
235182_PM_at	AI816793	ISM1	isthmin 1 homolog (zebrafish)	5.54	4.53	-1.00	0.00852	0.01052
208719_PM_s_at	U59321	DDX17	DEAD (Asp-Glu-Ala-Asp) box polypeptide 17	9.03	8.02	-1.01	0.01500	0.01539
208151_PM_x_at	NM_030881	DDX17	DEAD (Asp-Glu-Ala-Asp) box polypeptide 17	9.38	8.37	-1.01	0.01152	0.01259
205399_PM_at	NM_004734	DCLK1	doublecortin-like kinase 1	7.70	6.67	-1.03	0.03105	0.02870
218730_PM_s_at	NM_014057	OGN	osteoglycin	5.44	4.35	-1.09	0.03972	0.01478
206172_PM_at	NM_000640	IL13RA2	interleukin 13 receptor, alpha 2	7.16	6.02	-1.14	0.03670	0.03408
206176_PM_at	NM_001718	BMP6	bone morphogenetic protein 6	7.10	5.97	-1.14	0.03339	0.01775
1558378_PM_a_d	BC004283	AHNAK2	AHNAK nucleoprotein 2	9.61	8.47	-1.15	0.00009	0.00009
208396_PM_s_a	NM_005019	PDE1A	phosphodiesterase 1A, calmodulin-dependent	7.81	6.66	-1.16	0.01221	0.02972
222722_PM_at	AV700059	OGN	osteoglycin	6.17	5.00	-1.17	0.03798	0.02058
210367_PM_s_at	AF010316	PTGES	prostaglandin E synthase	9.10	7.93	-1.17	0.03073	0.00715
213816_PM_at	AA005141	MET	met proto-oncogene (hepatocyte growth factor receptor)	7.68	6.48	-1.21	0.00474	0.00128
208609_PM_s_a	NM_019105	TNXB	tenascin XB	7.67	6.38	-1.30	0.04043	0.02516
216333_PM_x_at	M25813	TNXB	tenascin XB	8.50	7.19	-1.30	0.04545	0.02515
1558680_PM_s_d	BC894022	PDE1A	phosphodiesterase 1A, calmodulin-dependent	8.07	6.76	-1.31	0.00904	0.02333
203407_PM_at	NM_002705	PPL	periplakin	8.59	7.25	-1.34	0.00556	0.02714
227242_PM_s_a	BF592034	EBF3	early B-cell factor 3	6.91	5.57	-1.34	0.00506	0.00510
206093_PM_x_a	NM_007116	TNXA # TNXB	tenascin XA pseudogene # tenascin XB	8.29	6.85	-1.44	0.02777	0.01369
213451_PM_x_at	BE044614	TNXA # TNXB	tenascin XA pseudogene # tenascin XB	8.74	7.29	-1.46	0.03398	0.01774
203815_PM_at	NM_000853	GSTT1	glutathione S-transferase theta 1	8.48	6.96	-1.51	0.01804	0.01345
228635_PM_at	AI640307	PCDH10	protocadherin 10	5.86	4.13	-1.73	0.00154	0.00057

Supplemental Material 3. Continued



## Supplemental Material 4. mRNA expression profile differences between fibroblasts from MDD and CNTRL subjects.

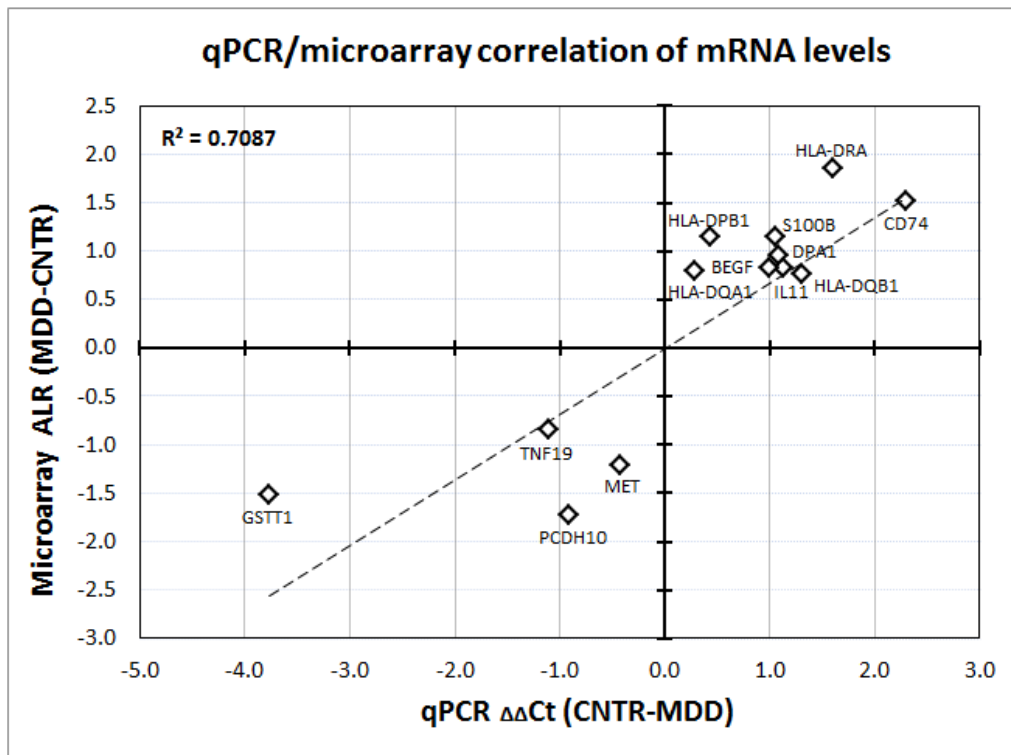
Two-way unsupervised hierarchical clustering was performed on the Log 2 expression levels of 162 differentially expressed mRNAs. Samples were clustered vertically, mRNAs were clustered horizontally. Each colored square represents a normalized gene expression level, color coded for increase (red) or decrease (blue) from the mean. Color intensity is proportional to magnitude of change. Alphanumerical entries to the right of the column denote microarray probe sets and gene symbols. The clustering resulted in a separation of the majority of samples that was related to the diagnostic condition (vertical dendrogram: green - CNTR samples, purple - MDD samples). For more detail, see Supplemental Material 3.



### Supplemental Material 5. Microarray data validation by qPCR.

qPCR analyses were used to independently test the expression level of 14 mRNAs. The Ct values for each of them was normalized to the GAPDH Ct value and the difference between CNTR and MDD was measured by  $\Delta\Delta Ct$  ( $\Delta\Delta Ct = \Delta Ct_{CNTR} - \Delta Ct_{MDD}$ ). Microarray expression differences measured by ALR (y-axis) were correlated to the qPCR differences measured by  $\Delta\Delta Ct$  (x-axis).

Gene symbol	qPCR ddCT	qPCR pVal	MA ALR	MA pVal
CD74	2.29	0.012	1.51	0.049
HLA-DRA	1.61	0.017	1.86	0.048
HLA-DQB1	1.31	0.018	0.76	0.043
IL11	1.13	0.017	0.83	0.019
DPA1	1.08	0.011	0.96	0.037
S100B	1.05	0.031	1.14	0.037
BEGF	1.00	0.010	0.83	0.031
HLA-DPB1	0.43	0.156	1.15	0.036
HLA-DQA1	0.29	0.285	0.80	0.041
MET	-0.42	0.043	-1.21	0.001
PCDH10	-0.91	0.036	-1.73	0.002
TNF19	-1.11	0.007	-0.84	0.015
GSTT1	-3.77	0.007	-1.51	0.013



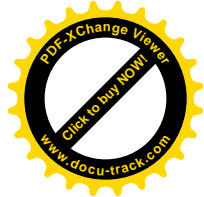
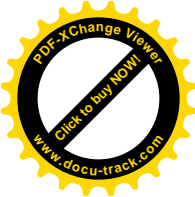




of

miRNA ID	ddCt D-C	<i>p</i> -value
hsa-miR-122	2.17	0.00004
hsa-miR-32	2.01	0.02137
hsa-miR-196b*	1.96	0.02807
hsa-miR-377	1.62	0.01040
hsa-miR-193a-3p	1.52	0.01756
hsa-miR-337-5p	1.52	0.00428
hsa-miR-675*	1.46	0.00648
hsa-miR-3176	1.39	0.01719
hsa-miR-21*	0.91	0.03960
hsa-miR-22	0.76	0.04233
hsa-miR-425*	0.71	0.02273
hsa-miR-185	0.60	0.00380
hsa-miR-296-5p	0.56	0.01870
hsa-miR-103a	0.55	0.01982
hsa-miR-107	0.53	0.03574
hsa-miR-186	0.53	0.03432
hsa-miR-887	0.45	0.02768
hsa-miR-132	-0.42	0.00278
hsa-miR-421	-0.43	0.00129
hsa-miR-542-3p	-0.44	0.00783
hsa-miR-450a	-0.50	0.02326
hsa-miR-16-2*	-0.54	0.03806
hsa-miR-424	-0.69	0.03091
hsa-miR-628-3p	-0.72	0.01009
hsa-miR-629	-0.76	0.02441
hsa-miR-4293	-0.77	0.00858
hsa-miR-661	-0.80	0.00724
hsa-miR-3909	-0.80	0.02860
hsa-miR-33a*	-0.80	0.01558
hsa-miR-135b	-0.84	0.02895
hsa-miR-7	-0.96	0.03198
hsa-miR-4267	-0.97	0.03604
hsa-miR-548aa	-1.05	0.00520
hsa-miR-548d-3p	-1.25	0.01201
hsa-miR-613	-1.53	0.00250
hsa-miR-3714	-1.58	0.02024
hsa-miR-1294	-1.78	0.03714
hsa-miR-429	-2.00	0.01091

**Supplemental Material 6.**  
**miRNA changes between fibroblasts originating from MDD patients and healthy controls.**  
 Positive  $\Delta\Delta Ct$  values denote miRNA downregulation in MDD fibroblasts (17 miRNAs), negative values correspond to the magnitude upregulation (21 miRNAs).



## Supplemental Material 7. Differentially expressed miRNAs in MDD fibroblasts and their predicted mRNA targets (TargetScan).

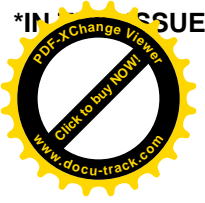
### A. Downregulated miRNAs in MDD and their putative mRNA expression targets (TargetScan)

miRNA ID	ddCt D-C	p-value	# of mRNA targets	mRNA up in MDD	mRNA down in MDD	# mRNAs up	# mRNAs down
hsa-miR-122	2.17	0.0000	172	---	FOXP2, CBL, OCLN, MASP1	0	4
hsa-miR-32	2.01	0.0214	306	BCL11A	IL6ST, SSFA2, PAX3, PCDH10	1	4
hsa-miR-196b*	1.96	0.0281	38	---	---	0	0
hsa-miR-377	1.62	0.0104	566	---	SEMA3D, LSAMP, RALGPS2, DCLK1, ERC1, RASSF8, NFIB, CBL, PCDH10	0	9
hsa-miR-193a-3p	1.52	0.0176	207	---	SLC23A2, FAIM2, ETV1,	0	3
hsa-miR-337-5p	1.52	0.0043	14	---	---	0	0
hsa-miR-675*	1.46	0.0065	4	---	---	0	0
hsa-miR-3176	1.39	0.0172	179	---	SLC23A2, KCNJ2	0	2
hsa-miR-21	0.91	0.0396	164	BCL11A	PIK3R1, RALGPS2	1	2
hsa-miR-22	0.76	0.0423	508	SLC2A1	FMNL2, ETV1, NFIB, CBL, OGN	1	5
hsa-miR-425*	0.71	0.0227	212	---	ZFHX4, CBL, XPNPEP3	0	3
hsa-miR-185	0.60	0.0038	188	---	NFIB	0	1
hsa-miR-296-5p	0.56	0.0187	172	---	---	0	0
hsa-miR-103a	0.55	0.0198	636	FRMD4A, BCL11A	PIK3R1, PER3, DCLK1, KLF4, FGF18, RASSF8, NFIB, SVEP1, ZCCHC2	2	9
hsa-miR-107	0.53	0.0357	14	---	---	1	3
hsa-miR-186	0.53	0.0343	849	FRMD4A	SLC23A2, FOXP2, KIAA1324L, NFIB, OCLN, AFF1	1	6
hsa-miR-887	0.45	0.0277	10	---	---	0	0

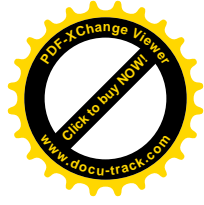
### B. Upregulated miRNAs in MDD and their putative mRNA expression targets (TargetScan)

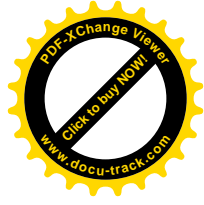
miRNA ID	ddCt D-C	p-value	# of mRNA targets	mRNA up in MDD	mRNA down in MDD	# mRNAs up	# mRNAs down
hsa-mir-132	-0.42	0.0028	261	SLC2A1	ETV1, ANKRD29	1	2
hsa-mir-421	-0.43	0.0013	426	---	RAPGEF2, NFIB, CBL, DDX17	0	4
hsa-mir-542	-0.44	0.0078	286	---	LSAMP, ZFHX4, CBL	0	3
hsa-mir-450a	-0.50	0.0233	9	---	---	0	0
hsa-mir-16	-0.54	0.0381	387	---	SEMA3D, HECTD1, ATP7A, RASSF8, SVEP1, ZCCHC2	0	6
hsa-mir-424	-0.69	0.0309	175	---	ZFHX4	0	1
hsa-mir-628-3p	-0.72	0.0101	112	---	DCLK1, AMPD3	0	1
hsa-mir-629-5p	-0.76	0.0244	196	---	ERAP1	0	1
hsa-mir-4293	-0.77	0.0086	189	SLC2A1	XPNPEP3	1	1
hsa-mir-661	-0.80	0.0072	319	---	IGF2BP3, NFIB, CBL,	1	3
hsa-mir-3909	-0.80	0.0286	186	---	CHM, CBL, PTGFRN	1	3
hsa-mir-33a	-0.80	0.0156	417	---	ZFHX4, DST, DCLK1, ERC1, RASSF8, CPT1A, PTGFRN, PCDH10	0	8
hsa-mir-135b	-0.84	0.0289	69	BCL11A	MASP1	1	1
hsa-mir-7	-0.96	0.0320	444	---	ZBTB38, KLF4, NFIB, KCNJ2	0	4
hsa-mir-4267	-0.97	0.0360	442	---	ZFHX4, DST, DCLK1, ERC1, RAPGEF2, RALGPS2, AFF1	0	7
hsa-mir-548a-3p	-1.05	0.0052	706	SCG2, B3GNT7, SLC2A1, FRMD4A, BCL11A	SLC23A2, PIK3R1, LSAMP, ZFHX4, FOXP2, RAPGEF2, IL1R1, NFIB, ERAP1	5	9
hsa-mir-548d-3p	-1.25	0.0120	145	---	FOXP2, PCDH10	0	2
hsa-mir-613	-1.53	0.0025	240	---	CHM, DDX17	0	2
hsa-mir-3714	-1.58	0.0202	1276	FRMD4A	DNAJC13, RALGPS2, PER3, ERC1, KLF4, ATP7A, RAPGEF2, ETV1, AMPD3, RASSF8, EBF3, KIAA1324L, NFIB, CPT1A, CBL, ENPP4, AFF1, KCNJ2, BMP6	1	19
hsa-mir-1294	-1.78	0.0371	298	RUFY2, FRMD4A	SEMA3D, NFIB, CBL	2	3
hsa-mir-429	-2.00	0.0109	237	FRMD4A	RAPGEF2, RASSF8, CBL, OCLN	2	7

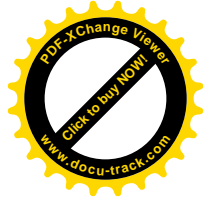
LEGEND: Red lettering - upregulated mRNAs in MDD; Green lettering - downregulated mRNAs in MDD

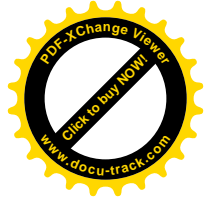


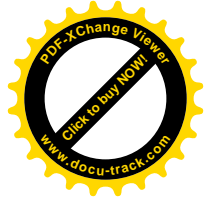
Cultured fibroblasts from patients with Major Depressive Disorder and matched controls were assayed for mRNA and miRNA expression. MDD fibroblasts showed a strong mRNA gene expression change in molecular pathways related to cell-to-cell communication, innate/adaptive immunity and cell proliferation. Furthermore, the same patient fibroblasts showed altered expression of a distinct panel of miRNAs. The data suggest that a combined miRNA-mRNA analyses of dermal fibroblasts provide insights into the molecular mechanisms associated with brain disorders.



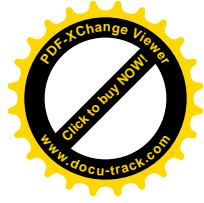


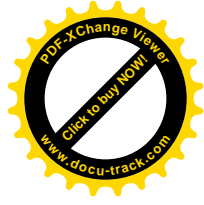












Manuscript Submission Form RCS  
[Click here to download Manuscript Submission Form: MSF-RCS.pdf](#)

